# Transfection efficiency in rat soleus and SERCA1b expression in human skeletal muscles

Ph.D. Thesis

Magdolna Kósa MD

Supervisor: Dr. Ernő Zádor

Department of Biochemistry

Faculty of General Medicine

University of Szeged

2014

Szeged

**Articles related to the subject of the thesis:**

I. **M. Kósa**, E. Zádor (2013) Transfection Efficiency Along the Regenerating Soleus Muscle of the Rat. *Mol Biotechnol* 2013 54(2):220-7.
   IF: 2.262

II. V. Guglielmi, G. Vattemi, F. Gualandi, N. C. Voermans, M. Marini, C. Scotton, E. Pegoraro, A. Oosterhof, **M. Kósa**, E. Zádor, E. M. Valente, D. De Grandis, M. Neri, V. Codemo, A. Novelli, T. H. van Kuppevelt, B. Dallapiccola, B. G. van Engelen, A. Ferlini, G. Tomelleri (2013) Serca1 protein expression in muscle of patients with Brody disease and Brody syndrome and in cultured human muscle fibers. *Mol Genet Metab* 110(1-2):162-9.
   IF: 2.834

III. **M. Kósa**, K. Brinyiczki, P. van Damme, N. Goemans, K. Hancsák, L. Mendler, E. Zádor (2014) The neonatal sarcoplasmic reticulum $Ca^{2+}$-ATPase gives a clue to development and pathology in human muscles. (submitted)

# Table of Contents

# LIST OF ABBREVIATIONS

| | |
|---|---|
| **AChE** | acethylcholinesterase |
| **ANOVA** | analysis of variance |
| **BAT** | brown adipose tissue |
| **BCA** | bicinchoninic acid |
| **cDNA** | complementary DNA |
| **CMV** | cytomegalo virus |
| **CTL** | cytotoxic T-lymphocyte |
| **CSA** | cross sectional area |
| **DEP** | diethyl pyrocarbonate |
| **DHPR** | dihydropyridine receptor |
| **DM1** | myotonic dystrophy type 1 |
| **DM2** | myotonic dystrophy type 2 |
| **DMD** | Duchenne muscular dystrophy |
| **dnRAS** | dominant negative Ras |
| **DsRed** | discosoma red |
| **ec.** | extracellular |
| **ECF** | enhanced chemifluorescence |
| **ECL** | enhanced chemiluminescence |
| **EDL** | extensor digitorum longus muscle |
| **EGFP** | enhanced green fluorescent protein |
| **ER** | endoplasmic reticulum |
| **EthBr** | ethidium bromide |
| **FITC** | fluorescein isothiocyanate |
| **HEPES** | 4-(2-Hydroxyethyl)piperazine-1-ethanesulfonic acid sodium salt |
| **ic.** | intracellular |
| **$I_{CRAC}$** | $Ca^{2+}$-release activated channel current |
| **IP3-R** | inositol trisphosphate-3 receptor |
| **IQR** | interquartile range |
| **MBNL** | muscleblind-like protein |
| **mRNA** | messenger RNA |
| **MTJ** | myotendonal junction |

| | |
|---|---|
| **NFATc1** | nuclear factor of activated T-cells cytoplasmic 1 |
| **NME** | neuromuscular end-plate |
| **NMJ** | neuromuscular junction |
| **ODu** | optical data unit |
| **PBS** | phosphate buffered saline |
| **PCR** | polymerase chain reaction |
| **PGF** | prostaglandin F |
| **pDsRed** | plasmid coding discosoma red protein |
| **pEGFP** | plasmid coding enhanced green fluorescent protein |
| **PM** | plasma membrane |
| **RIPA** | radio immunoprecipitation assay |
| **RNAi** | RNA interference |
| **RO** | rhodamine |
| **RyR** | ryanodine receptor |
| **SDS** | sodium dodecyl sulfate |
| **SEM** | standard error of the mean |
| **SERCA** | sarco/endoplasmic reticulum $Ca^{2+}$-pump |
| **siRNA** | small interfering RNA |
| **SOCE** | store operated calcium entry |
| **SR** | sarcoplasmic reticulum |
| **STIM** | stromal interaction molecule |
| **TA** | tibialis anterior muscle |
| **TnT** | troponin T |
| **TRPC** | transient receptor potential channel |

**INTRODUCTION**

*Transfection of skeletal muscle*

Transfection is a method for delivering foreign genes to eukaryotic cells in order to make them transgenic. Transfection of skeletal muscle is applied in a growing field of research; besides attempts for gene therapy of muscle diseases, transgenic muscle is also used for attaining secretion of foreign proteins.

Systemic secretion of foreign proteins can lead to novel therapies for patients lacking elementary processes such as the synthesis of blood clotting factor VII in haemophilia A [1], factor IX in haemophilia B [2], or erythropoietin [3, 4]. Transgenic proteins synthesized by skeletal muscle like hypoxia inducible factor-1 (HIF-1) or hem oxygenase-1 can be cardioprotective [5, 6], while transgenic muscle decorin improved TGF-β1 induced fibrotic kidney disease [7]. Examples for systemic response to skeletal muscle transgenesis are DNA vaccines, by which the protein of the pathogen is presented on the transfected cells by MHCI thereby activating cytotoxic T-lymphocytes (CTL). The most modern vaccines often contain recombinant proteins that are synthesized in cells performing different posttranslational modifications  than human cells do therefore these proteins are not detected by human MHCI molecules and do not activate CTLs. DNA vaccines (having been introduced to human muscle) can overcome these hindrances [8].

Transfections to correct skeletal muscle malfunctions (therapy) also represent a huge field. A recent approach for instance expressed adiponectin and palliated skeletal muscle dysfunction in type 2 diabetes [9]. Another one expressed the Sonic hedgehoc morphogen and improved age-related impairment of muscle regeneration [10]. Furthermore angiogenesis in chronic limb ischemia has been achieved with FGF-1 expression in animal experiments and clinical trials [11, 12].

There are several purposes to use gene delivery for experimental and therapeutic purposes in skeletal muscle. Viral or non-viral gene transfer is a matter in issue (reviewed by [13] and [14]). Successful transfection of regenerating skeletal muscle can be achieved by naked plasmid injection without any supplementary techniques [15]. However transfection efficacy is very low in this case since plasmids have to overcome several

hindrances while reaching myonuclei, and still have to remain in proper condition. These obstacles are extracellular DNAses, quick drainage via lymphatic pathways, entrance to the cytoplasm and transport to the nucleus. Because of the benefits of non-viral applications several methods have been developed and large efforts have been made to improve transfection efficiency of the above method. Technics utilised electroporation [16], intramuscular application of hyaluronidase [17, 18], ultrasound treatment [19], polymer addition [20, 21], gene gun approach [22] and hydrodynamic plasmid delivery [23].

Despite all attempts the transfection still remained below the optimal efficiency. However there are certain plasmids - encoding dominant negative Ras (dnRas) or the siRNA of the neonatal form of sarco/endoplasmic $Ca^{2+}$-ATPase 1 (SERCA1b) - whose simple injection in 20% sucrose improves muscle weight and fibre size of the whole rat soleus muscle during regeneration [24, 25]. This kind of transfection is only successful in regenerating muscle. Regeneration can be achieved by treating skeletal muscles with an appropriate dose of notexin, the toxin of the of the Australian tiger snake (Notechis scutatus scutatus) venom. Notexin has myotoxic and neurotoxic effects [26, 27]. The intramuscular injection of the toxin results in almost complete myofibre damage [28, 29] while the surrounding basal lamina, satellite cells and microcirculation is left intact enabling rapid reconstruction of myofibres along the entire muscle [26, 30-32]. It has been shown that approximately 1% of the fibres are transfected at the place of plasmid injection in the notexin treated soleus [25]. Because of the remarkable stimulation of muscle growth in the whole regenerating muscle by dnRas or SERCA1b RNAi transfection the question risen was: has the transfection efficiency indeed been so low (around 1 %) as expected? When investigating transfection efficiency, many articles compare cross sections from certain parts of the muscle [17, 18] or measure the amount of the expressed transgenic protein in the whole muscle homogenate [21, 33]. Both of these methods have drawbacks: the transversal sections reveal transfection in a limited part of the muscle, while measuring the transgenic protein in the whole muscle homogenate provides no information of transgene distribution and morphological effects. In spite of these, only a few laboratories have investigated transfection efficiency on longitudinal sections [34] and in whole mount preparations of mice muscles [33-35]. They showed that the expression of the transgene was restricted to the place of transfection; meanwhile others

found that after injection of plasmid into single fibres, the expressed GFP diffused along the whole fibre [36]. Although these results come from mice, which have shorter muscles than rats, they still show variance. Therefore it is relevant to study the change of transfection efficiency along muscles of larger animals, i.e. rats. In connection with this, we also aimed to study the fibre length in the regenerating soleus compared to that of the normal muscle. This question needs to be answered since the fibre length is nearly equal to muscle length in the young soleus [37] and the fibre length in regeneration could be much shorter therefore largely determine transfection efficiency along the soleus.

## $Ca^{2+}$ homeostasis of skeletal muscle

SERCA1b was one of the proteins whose inhibited expression at the transcript level by naked plasmid transfection resulted in increase of the whole muscle during regeneration. This protein is part of the machinery that reduces intracellular (ic.) $Ca^{2+}$ in skeletal muscle by transporting it to the sarcoplasmic reticulum on the cost of ATP molecules. The maintenance of low levels of resting ic. $Ca^{2+}$ is of particular interest since this ion takes part in two basic processes: muscle contraction and signal transduction. Contraction is triggered by acetylcholine (ACh) binding on nicotinergic Ach receptors. Depolarization induces ryanodine receptor (RyR) activation via dihydropyridine receptors (DHPR) of T-tubuli. This results in elevated ic. $Ca^{2+}$-concentration, leading to muscle contraction. During the process sarcoplasmic reticulum $Ca^{2+}$ stores are almost but not completely depleted – residual $Ca^{2+}$ increases by age [38]. The extent of $Ca^{2+}$-signal is not only sufficient for contraction but it in certain cases it is also enough for nuclear transposition of the calcineurin activated NFATc1 which shifts transcription toward slow skeletal muscle genes [39, 40]. However, RyR activation induced $Ca^{2+}$-transients are too short to sustain the nuclear localisation of NFATc1. Not so the non-voltage dependent $Ca^{2+}$-influx from the ec. space via TRPC3 channels (transient receptor potential channel) which results in a prolonged signal that together with RyR activation is already capable of stabilising the nuclear position of NFATc1, allowing its transcription factor function [39]. TRPC3 activation is a part of the so called store operated calcium entry (SOCE) (SOCE reviewed by [41-43]. The mechanism of SOCE was first described in non-excitable cells where STIM1 and STIM2 (stromal interaction molecule) are stabilized in the ER

membrane by $Ca^{2+}$-binding of its EF-hand motif at the luminal site. Upon store depletion STIM molecules also lose their $Ca^{2+}$, this enables them to oligomerize in the ER membrane, and translocate to punctuate structures near the PM, which are referred to as ER-PM junctions. The final step of this process is the activation of Orai proteins, that are plasma membrane $Ca^{2+}$-channels responsible for the $Ca^{2+}$-release activated channel current ($I_{CRAC}$) [41, 44-46].
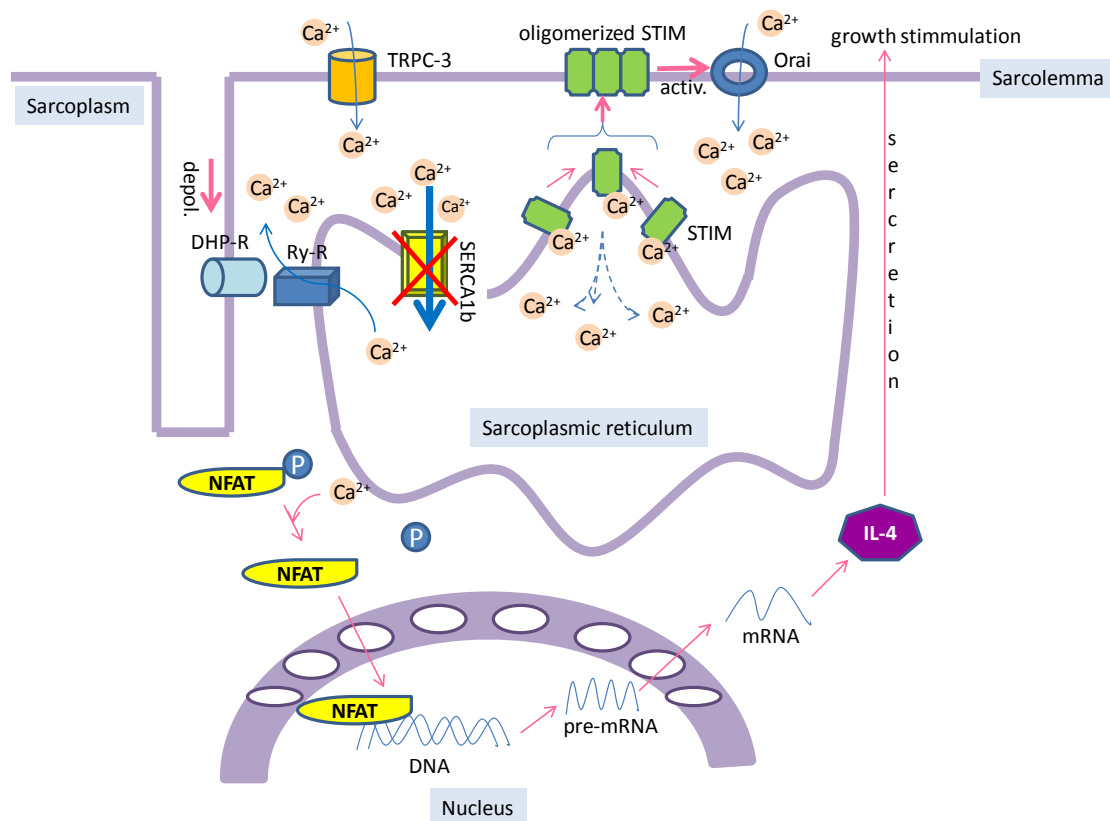


*Figure 1: The suggested role of SERCA1b. Depolarization induces a change in DHPR conformation which in turn opens RyRs. This results in rapid depletion of SR $Ca^{2+}$ stores that activates the store operated $Ca^{2+}$ entry pathways. STIM molecules in the SR membrane lose their luminal bound $Ca^{2+}$ which enables their oligomerization and afterwards transposition to the sarcolemma, where they activate the Orai channels and extracellular $Ca^{2+}$ influx [41, 44-47]. Another part of SOCE are TRPC-3 channels, that also induce an inward $Ca^{2+}$ current due to SR store depletion [39]. The latter mechanism can achieve a more prolonged $Ca^{2+}$ signal than RyRs and enable transposition of NFATc1 from the sarcoplasm to the nucleus (via dephosphorylating*

*calcineurin) where it induces transcription of IL-4. IL-4 is secreted into the extracellular space as paracrine muscle growth factor [42, 48]. SERCA1b as the major Ca$^{2+}$ pump of the SR membrane might play an essential role in refilling SR stores. This is supported by RNAi silencing of SERCA1b in a few fibres, which leads to IL-4 secretion and autocrine/paracrine growth of the whole regenerating muscle. This effect of RNAi can be prevented by calcineurin inhibition [25].*

Recent results have confirmed the presence of STIM1 in myotubes and adult skeletal muscle as well [47]. Myocytes lacking STIM1 have reduced SR Ca$^{2+}$-content, myotubes of STIM1$^{-/-}$ mice have reduced SERCA1 content and increased sarcolipin content which is a potent inhibitor of SERCA1 function. It seems that the SOCE-sarcolipin relation also works vice versa: absence of sarcolipin augmented SOCE but without changing SERCA1 or calreticulin expression. The antagonistic effects of sarcolipin and STIM1 seem to be well equilibrated during development since sarcolipin is primary expressed during embryonic development, whose place is taken over by the postnatal upregulated STIM1. Therefore sarcolipin delays SR maturation and the expression of several slow muscle expressed genes like slow troponin, myoglobin, and NFATc1 [49].

Other factors that influence free Ca$^{2+}$-levels in different compartments are *1) Ca$^{2+}$-binding proteins.* These have important role in cytoplasmic Ca$^{2+}$-mediated signal cascades like calmodulin [50] or Ca$^{2+}$-buffering in ER/ SR like calreticulin, calsequestrin, sarcalumenin [51-53] which bind Ca$^{2+}$ and therefore reduce free cytosolic/SR Ca$^{2+}$-levels; *2) Pumps* responsible for elimination of Ca$^{2+}$ in a certain compartment. Plasma membrane (PM) Ca$^{2+}$-ATPase and Na$^{+}$/Ca$^{2+}$-exchanger also in the PM act by reducing cytosolic Ca$^{2+}$, while SERCA1 in the SR membrane accumulates Ca$^{2+}$ in the SR lumen. Silencing SERCA1b (by siRNA) results in sustained elevation of sarcoplasmic Ca$^{2+}$, enabling NFAT transposition into the nucleus and paralleled by IL-4 secretion. This latter is however suspended by transfection with plasmids coding for the calcineurin inhibitor. Therefore it seems that SERCA1b inhibition and calcineurin (a Ca$^{2+}$-dependent serine/threonine phosphatase) act on the same way by increasing skeletal muscle mass during regeneration [25].

The sarco/endoplasmic reticulum $Ca^{2+}$-ATPases are responsible for the reduction of the sarco/cytoplasmic $Ca^{2+}$-concentration as part of the decay of excitatory cell responses. There are three SERCA genes in mammals (named atp2a1, atp2a2 and atp2a3, coding SERCA1, SERCA2 and SERCA3 subsequently), each can code for more than one transcript and corresponding protein isoform. The fast twitch and slow twitch/cardiac muscle specific SERCA1a and SERCA2a were first identified at the transcript level [54]. However one splice isoform of SERCA2, the SERCA2b is almost ubiquitously present in many non-muscle tissues [55]. The third SERCA gene, coding SERCA3 is not muscle specific; its cDNA was cloned from rat kidney. It showed 75-77% identity with fast-twitch and slow-twitch/cardiac isoforms [56]. Though skeletal muscle specific SERCAs are mostly related to certain fibre types, they are alone not the best markers for fibre typing. Several muscles contain hybrid fibres whose composition considering SERCA and myosin heavy chain isoforms is changing according to muscle type and species [57].
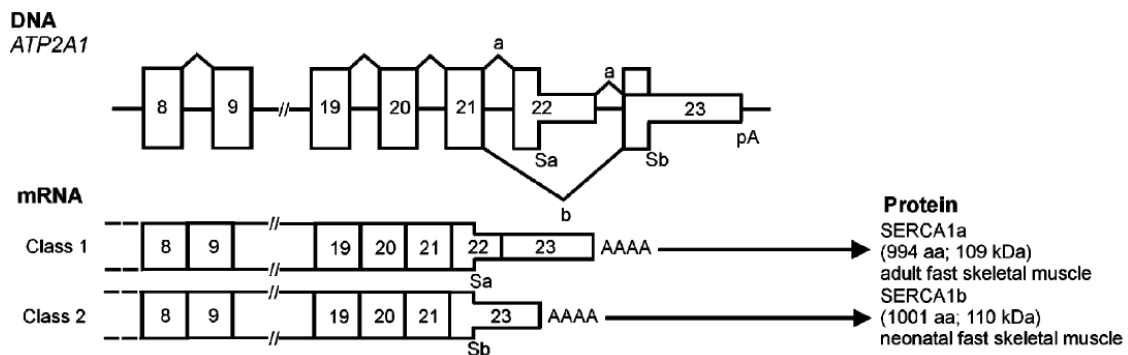


*Figure 2: The muscle specific SERCA1 isoforms [55].*

*Expression of SERCA1 isoforms:* The gene of SERCA1 (atp2a1) encodes several isoforms resulted by development and tissue dependent splicing of the main transcript. In the two truncated SERCA1s (S1Ts) exon 11 and/or exon 4 are spliced out forming a shorter protein with no $Ca^{2+}$-pump activity and no expression in muscle [58]. A non-muscle tissue, the brown adipose tissue (BAT), is common in fetal age and also expresses a SERCA molecule that may react with SERCA1 antibody. Latest results have proved the direct involvement of SERCA1 in thermogenesis in rat BAT [59] where fusion of

mitochondrial and ER membranes – both containing SERCA1 - has already been confirmed [60, 61]. The non-truncated isoforms are expressed in adult fast (SERCA1a) and in neonatal/developing (SERCA1b) skeletal muscle [62, 63]. The rate of the neonatal splice variant decreased from the foetal 72% to 4% in adult animals [54] exhibiting a developmentally regulated alternative splicing of SERCA1. The age of animals investigated has a significant impact on the expressed SERCA1 isoform, so the deduced amino acid sequence was referred to SERCA1a as the rat SERCA1 has been cloned from cDNA library of adult animals [64]. SERCA1a and 1b proteins are almost identical in human and rat. The differentiation between SERCA1a and SERCA1b proteins is only possible with antibodies produced against the C-terminal octapeptide of the SERCA1b molecule [63]. In regenerating rat soleus and EDL, the SERCA1b protein expression follows the changes in the mRNA level with one-two days delay; but in passively stretched muscle only the mRNA is elevated without SERCA1b protein expression. This shows that while the splicing can be upregulated the translation of SERCA1b is somehow blocked in non developing adult muscles. The SERCA1b protein dominates over SERCA1a in mouse neonatal diaphragm [63] and this is especially interesting since SERCA1-null mice (deficient for both SERCA1a and 1b) showed uneven development of diaphragm and died in progressive respiratory failure soon after birth without the compensatory up-regulation of other SERCA isoforms [65].

The SERCA1b protein is present only in neonatal and regenerating muscle [29, 63, 66], and its inhibition by siRNA had significant impact on regeneration of the rat soleus. However the expression of this $Ca^{2+}$ pump has not been studied thoroughly only preliminary in developing human muscles at perinatal age [67].


*Altered intracellular calcium concentration and muscle pathology – diseases*

Disturbed $Ca^{2+}$-homeostasis is common in Duchenne muscular dystrophy (DMD) and pronounced elevation of SERCA1b transcript has already been described in myotonic dystrophies (DM, [68]), especially in the type 2 (DM2).

DMD is a progressive, typical degenerative-regenerative disorder, with intensive regeneration process that is exhausting by time. DMD muscles lack dystrophin whose

association with the triadic junctions first brought the idea of affected $Ca^{2+}$-regulation in this disease [69]. Resting ic. $Ca^{2+}$ is unquestionably increased in mdx myotubes and muscle fibres that results in a membrane potential partially shifted towards depolarization [70, 71]. This has been shown to be a consequence of three main factors: 1) sarcolemmal $Ca^{2+}$-leak, 2) SR $Ca^{2+}$-leak, 3) altered $Ca^{2+}$-buffering proteins, 4) impaired SR filling. Abnormal reaction to long term contraction leads to frequent sarcolemma disruptions in dystrophin deficient fibres whereby $Ca^{2+}$-leak channel activity is augmented, increasing resting cytoplasmic $Ca^{2+}$ [70, 72, 73]. Mechanosensitive cation channels (TRPC1) are not down-regulated during development of mdx mice as in the control and may also contribute to stress induced $Ca^{2+}$-entry from ec. space by their increased number and activity [74]. Additionally TRPC3 overexpressing transgenic mice also show clinical signs of DMD [75]. $Ca^{2+}$-leak of SR also contributes to increased resting $Ca^{2+}$ via RyR and IP3 receptors [71]. Heterogeneous results appeared about $Ca^{2+}$-binding proteins like calsequestrin and sarcalumenin which were reduced in dystrophic fibres of mdx mice, while calmodulin was left unaffected [76]. Others found that cytosolic calmodulin was decreased and calsequestrin increased in affected muscles of mdx mice, and both proteins were reduced in diaphragm while increased in extraocular muscles [77]. The variations considering for example calsequestrin expression could be due to muscle specific differences. This turned out also in another study, where the calsequestrin content of wild type and mdx mice of tibialis anterior (TA) and EDL muscles showed no significant difference, while there was a decrease in the soleus and an increase in the intrinsic laryngeal muscle [78]. Investigation of $Ca^{2+}$-handling proteins in different muscles is of particular importance since certain muscles are spared in these patients. Laryngeal, extraocular and toe muscles are less affected. Comparison of these muscles with the affected ones is crucial whereby possible treatment could be developed. For instance, SERCA1 expression is increased in the spared intrinsic laryngeal muscles in Duchenne muscular dystrophy [78]. What is more, overexpression of SERCA1 in sarcoglycan or dystrophin null mice improved the dystrophic phenotype [79].

DM is accompanied by facial and distal limb weakness and myotonia. Clinical signs of muscle weakness are of different severity. Possible additional symptoms are insulin resistance and other endocrine abnormalities like testicular atrophy; cataracts, decay of cognitive functions, sleep disturbances (reviewed by [80]). There are two groups of

myotonic dystrophies, DM1 and DM2 which are linked to mutations on different genes (DM1- myotonic dystrophy protein kinase, DM2- zinc finger protein 9), however both genetic modifications are trinucleotide expansions leading to altered regulation of development dependent splicing [81-85]. Splicing of several mRNAs is disturbed in both conditions, like cardiac TnT, insulin-receptor, muscle specific chloride channel-1, myotubularin related protein-1 and SERCA1 [68, 85-88]. Therefore the SERCA1b expression is also interesting in this disease.

**AIMS**

Our plan was to explore different aspects of SERCA1b expression:

1) We wanted to clarify the exact ratio of transgenic muscle fibres after naked plasmid transfection in order to shed more light to the mechanism of the unexpectedly high growth stimulation of regenerating rat muscles after SERCA1b siRNA transfection.

2) Since experiments have shown the importance of SERCA1b in signalization of regenerating rodent muscle, our further aim was to describe expression of this neonatal $Ca^{2+}$ pump in developing human muscles.

3) We also wanted to fill the gap considering SERCA1b protein expression in diseased DMD, DM1 and DM2 muscles.

**MATERIALS and METHODS**

*Animal treatment and frozen sectioning*

Male Wistar rats (320-390 g) were treated as described by Zádor et al. [29]. In brief animals were anesthetized by intraperitoneal injection of 4 % chloral hydrate (1 ml/100 g bodyweight). After a small incision on the lateral side of the left hind limb the soleus muscle was explored and injected with 0.15 ml notexin (Sigma-Aldrich) in 100 μg/ml solution. After the brief surgery animals could move, eat and drink according to their demands. For transfection the soleus was re-explored 4 days after the notexin treatment and injected with a total volume of 50 μl plasmid (1 μg/μl, 20 % sucrose in DEP water) by Hamilton microsyringe. On the 11th day of notexin induced regeneration and 7 days after transfection, the muscles were dissected, fixed on small wooden sticks by thread, cooled in liquid nitrogen chilled isopentane and stored at -70°C. For AChE staining before the 11th day of regeneration muscles were removed on the 5th or 7th day after notexin treatment without plasmid injection; for SERCA1b detection this happened on the 5th day. Animals were killed with an overdose of chloral hydrate. Experiments with animals were approved by the Ethical Committee of Animal Treatment of the Medical Faculty of the University of Szeged.

For later determination of transfection efficiency, frozen soleus muscles were cut into 6 approximately equal segments. After embedding the segments in Tissue Tek, 10 μm thin frozen cross-sections were performed by Reichert-Jung Cryostat. For AChE staining cross sections as above and longitudinal sections of the same thickness were performed from the central third of the muscles. Native sections were air-dried on glass slides and stored on -25 °C until microscopic evaluation or staining.

*Plasmids*

pEGFP (3,4 kb) and pDsRed (3,3 kb) plasmids (Clontech) were used for transfection. Driven by CMV promoter they expressed green or red fluorescent proteins in muscle fibres which allowed direct investigation of transgene expression under fluorescent microscope.

*Calculating Transfection Efficiency*

Results presented here have been collected from 11 successfully transfected muscles from which 6 were injected with pEGFP, and 5 with pDsRed. An advantage of the green and red fluorescent proteins is the easy visualization without further staining procedures, difficulty in fibre identification presents only in extreme cases (very low emission versus background autofluorescence; high emission may result in light contamination of the surrounding fibres).

The number of transfected fibres was counted on 2-4 sections from each of the 6 segments on Nikon Labophot-2 fluorescent microscope (RO or FITC filter) equipped with Olympus DP71 camera connected to a computer with Cell* B imaging software. Fluorescent and light microscopic merged pictures were performed by Adobe Photoshop 7.0 CE.

*Staining of soleus sections*

Hematoxylin and eosin staining was performed to prove the stage of regeneration by measuring fibre cross sectional areas (CSA) and to count muscle fibres. Acetylcholinesterase histochemistry was prepared after Tago et al [89] but after washing sections with 3% $H_2O_2$, they were rinsed in PBS two times and incubated in ethopropazine ($2x10^{-4}M$) for 30 min in dark (as in [90]) to block unspecific cholinesterase activity. NMJs were counted under light microscope. Schematic drawings were prepared by MS Office PowerPoint 2007.

*Counting fibres associated with AChE positive staining*

AChE is bound to the basal lamina in the post-synaptic cleft [91, 92] and is an indicator of the neuromuscular junctions (NMJs). The other AChE-stained structures (i.e. myotendinous junctions and proprioceptors [93, 94]) have different morphology. AChE was stained on sections at least within 40-100 μm distance. Therefore at least 4 cross sections from each segment of six muscles were stained, and those with the highest number of AChE were selected and compared on diagrams.

Post mortem fetal and neonatal samples: 19 muscles of altogether 5 subjects (I-V.) were analyzed (permission received from the Ethical Committee of the University of Szeged). Brief summaries of the medical histories: **I.** intrauterine death, gestational age unknown, weight 1500 g; **II.** intrauterine death without known fetal or maternal cause, birth at the 30th gestational week; **III.** birth at 24th gestational week, death 2 months later, respiratory distress syndrome, necrotising enterocolitis, cerebral hemorrhage; **IV.** mature infant, death 2 and half weeks later, congenital heart disease followed by surgery; **V.** birth at 36th gestational week, death 1 month later, intrauterine infection and consequent sepsis. Investigated muscles: vastus lateralis, gluteus maximus, biceps brachii - later referred to as vastus, gluteus, biceps - and diaphragm.

Belgian DM2 and DMD samples: biopsies of two DM2 and three DMD patients were investigated (with permission of the Ethical Committee University Hospital Leuven). DM2 patients were 42 and 43 years old, samples were taken from the quadriceps muscle. Patients suffering from DMD were 7, 8 and 12 years old, had Calcort or Prednisone treatment in history, samples were taken from TA muscles.

Italian DM1, DM2 and control muscle samples: whole protein homogenates (equivalent with 100 µg total protein) of biopsies from altogether 12 adult patients were analyzed with the permission of the Ethical Committee of University of Verona. Samples were taken from the vastus lateralis muscle, and deltoid muscle in one case that belonged to a DM1 patient.

*RNA isolation and RT PCR*

RNA was isolated from muscles and reverse transcription was made as described in [29]. Primers for human SERCA1 (fw: 5'CTCCATCTGCCTCTCCATGTC3' and rev: 5'ATGCTCACTTCCTTCTTTCATCTT3') amplified a 248 bp and 206 bp fragment of SERCA1a and SERCA1b respectively as in [63]. Primers for human HPRT were 5'TGCTCGAGATGTGATGAAGG3' and 5'TCCCCTGTTGACTGGTCATT3' and amplified a 192 bp fragment in 33 cycles (95-60-72 $^{\circ}$C). PCR fragments were separated on 6 % PAGE, stained with EthBr and analyzed by GEL DOC 2000 (Bio-Rad).

The pcDNA3.1 plasmid expressing SERCA1b was co-transfected into COS-1 cells with EGFP expressing plasmid as described in [25]. After 2 days the transfected cells were harvested and extracted in lysis buffer as in [63] and analysed on immunoblot.

*Antibodies*

The mouse anti-SERCA1 monoclonal antibody (A3, cell supernatant) recognizes both SERCA1a and SERCA1b. These two isoforms differ significantly only in their C-terminal: $Gly_{994}$ of SERCA1a is replaced by the octapeptide 994-DPEDERRK-1001 in SERCA1b of human and rat as well. This enables specific distinction between the two molecules by antisera raised in rabbit against the SERCA1b C-terminal [63].

*Immunohistochemistry:*

10 μm thin consecutive frozen sections were stained for SERCA1b and SERCA1. Rat sections were handled as described previously [63] while human sections were treated with the difference that anti-SERCA1b antibody was used in 1:50 dilution.

*Western-blot*

Homogenates for gel loadings were prepared as described previously [95]. In brief muscles were homogenized in sucrose-HEPES lysis buffer (20 ml/g tissue) containing protease inhibitor coctail (Sigma Aldrich) and 1 mM PMSF. The non-soluble, mainly cytoskeletal components were pelleted at 1000 g, the supernatant was further centrifuged at 200 000 g to collect the microsomal membrane fraction in the pellet which was later suspended again and stored at -20 °C until use for SERCA Western-blot.

For homogenisation in RIPA solution (150 mM NaCl, 50 mM Tris-HCl (pH=7,5), 0,1 % Triton X 100, 0,1 % SDS, 25 mM sucrose) the buffer was supplemented with protease inhibitor cocktail (Sigma Aldrich) and 1 mM PMSF. After centrifuging at 1000 g homogenates were stored at -20 °C. Protein concentration of total homogenates was determined by the BCA method.

For preliminary analysis total homogenate of human muscles was run on gradient gels (8-16 % acrylamide in Tris-glycine, Pierce) and developed by ECL (Amersham) using SERCA1 (1:100) and SERCA1b (1:2000) primary antibodies.

Each gel loading of human samples was normalized to 5.5 mg fresh weight (indicated later if different). Loading series were designed in order to stay within linear detection range. On the gels increasing loadings of one sample was followed by decreasing loadings of another sample to maximize protein transfer to the membranes. Immunoblots were developed as in [63], shortly: membranes were first incubated with anti-SERCA1b serum (1:2000) and developed by ECF kit (Amersham) and detected on Typhoon Trio equipment. After a controlled time period (>24 hrs at 4 °C) when the fluorescence signal was bleached and the enzyme coupled to the $2^{nd}$ Ab also lost its activity, the same membrane was used for SERCA1 immunoblot (antibody dilution 1:100). The loading was checked by Ponceau S staining of the blots but this was informative only for the total extracts, since no SERCA bands were visible in the membrane-microsomal fraction and the other bands varied depending on the quality of post mortem samples. Therefore loading was controlled by equivalence to fresh weight. Band quantities (intensity · mm$^2$) were evaluated with Quantity One software (Bio-Rad). For determination of SERCA1a/SERCA1b ratio increasing loading series of a certain muscle were evaluated in parallel with the loadings of the 5 days regenerating rat soleus muscle on the same blot. SERCA1b/SERCA1 signal ratios were calculated for each loading of a muscle. Since these ratios may show variations at each loading, the real value of the SERCA1b/SERCA1 ratio was estimated from four increasing loadings of the investigated muscle by fitting a horizontal line with the method of least squares. The SERCA1b/SERCA1 ratio of the investigated muscle and the regenerating rat soleus were compared. No normalisation to internal control band was necessary because each loading was always related to the same regenerating rat muscle. The ratios of the investigated muscle and regenerating soleus (i.e. horizontal lines on graphs) were statistically compared by extra sum-of-squares F test (level of significance < 0,05). If ratios of two muscles were not significantly different, the graph showed one common line instead of two (e.g. in Fig. 11). Graphs and statistical analysis were performed by GraphPad Prism.

In transfection efficiency calculation comparison of the means were done by ANOVA and Bonferroni post-hoc test (Software: SPSS 15.0), data was presented by Sigma Plot 2000. Band intensities were evaluated with Quantity One software (Bio-Rad), graphs and calculations from Western-blot band contour quantities were prepared by Grahp Pad Prism (see above in "Western-blot"); presented data in "Results" correspond to mean band density $(ODu*mm^2) \pm SEM$; level of significance: $p < 0,05$.

## RESULTS:

*Transfection efficiency along the muscle*

Transfected fibres were distinguished from non-transfected ones by their high fluorescence, they stood alone or formed groups as it was reported by Doh et al. [35].
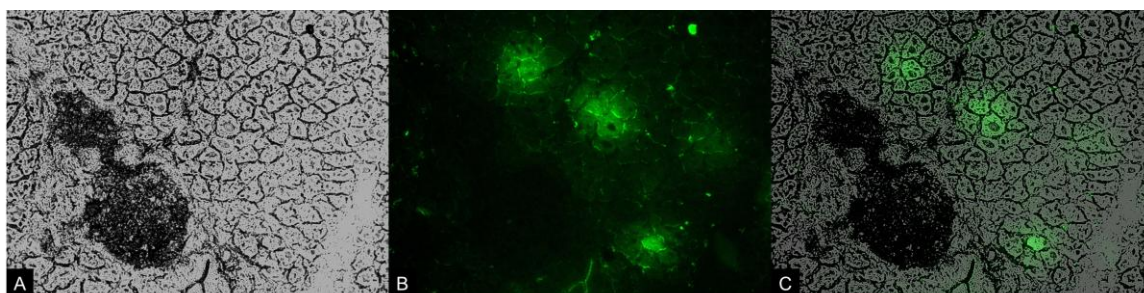


*Figure 3: Transfected fibres in groups are common around blood vessels. Gray-scale light microscope (A), fluorescent microscope (B) and merged (C) image (by photo editor software).*

Sections with the highest transfection rate were found in segments 2-4, and only one muscle had its peak transfection efficiency in the 5th segment. Data from the individual muscles (Table 1) also shows a decline in the number of transfected fibres toward the proximal and the distal ends. Summarizing the corresponding segments, 3rd and 4th segments after pEGFP injection, and 2nd, 3rd segments after pDsRed transfection contained significantly more transfected fibres compared to the first and the last segments (Fig. 4). This correlated well with the place of injections at the muscle mid-bellies.

| pEGFP | | Segments | | | | | pDsRed | | Segments | | | | |
|---|---|---|---|---|---|---|---|---|---|---|---|---|---|
| Muscle ID | **1** | **2** | **3** | **4** | **5** | **6** | Muscle ID | **1** | **2** | **3** | **4** | **5** | **6** |
| **a** | 8 | 13 | 6 | 4 | 2 | 3 | **g** | 0 | 12 | 10 | 26 | 11 | 0 |
| **b** | 5 | 13 | 51 | 49 | 22 | 6 | **h** | 8 | 18 | 31 | 11 | 6 | 0 |
| **c** | 1 | 8 | 11 | 17 | 44 | 11 | **i** | 13 | 335 | 22 | 9 | 2 | 0 |
| **d** | 0 | 21 | 86 | 39 | 9 | 0 | **j** | 8 | 37 | 38 | 49 | 21 | 1 |
| **e** | 6 | 19 | 40 | 20 | 0 | 0 | **k** | 3 | 23 | 26 | 10 | 11 | 4 |
| **f** | 0 | 0 | 10 | 9 | 4 | 3 | | | | | | | |

**Table 1** *Number of transfected fibres in the segments of 11 transfected muscles. Data represents average number of transfected fibres on cross sections. Muscles transfected with pEGFP or pDsRed are shown separately. Note that transfection efficiency is different in each muscle, but the number of transfected fibres declines toward the muscle ends.*

Associations were common around blood vessels (Fig. 3 A-C). Even fibres showing intensive fluoresce could stand alone, without any nearby transfected fibre.
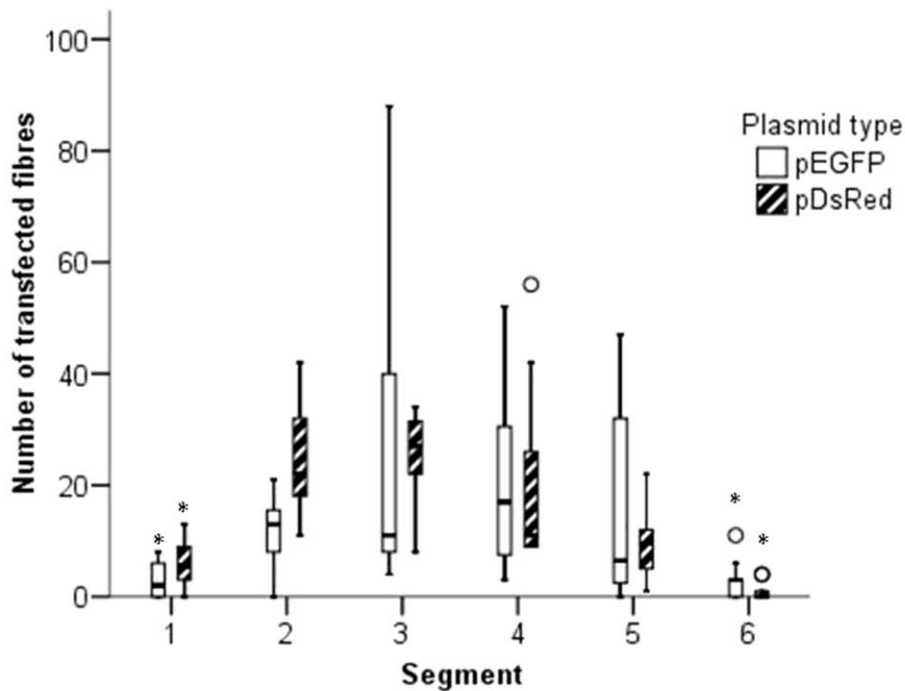


**Figure 4:** *Summary of transfected fibres in segments of 11 (pEGFP or pDsRed) transfected muscles. At each segment 2 vertical box plots demonstrate the transfected fibre counts. Empty boxes refer to muscles transfected with pEGFP, patterned ones to those with pDsRed. Length of boxes presents the interquartile range (IQR) computed from Tukey's hinges. Whisker caps*

indicate minimum and maximum values. Circles mark outlier values (more than 1.5 IQR's but less than 3 IQR's from the end of the box). There was no significant difference between pEGFP or pDsRed transfection efficiency within the same segment. Highest mean of transfected fibres is in segment 3 (both pEGFP and pDsRed). The peripheral segments 1 and 6 contain significantly less fibres than segment 3 and 4 in case of pEGFP transfection and segment 2 and 3 in case of pDsRed transfection.* marks significant differences (p< 0,05; Bonferroni post hoc test).
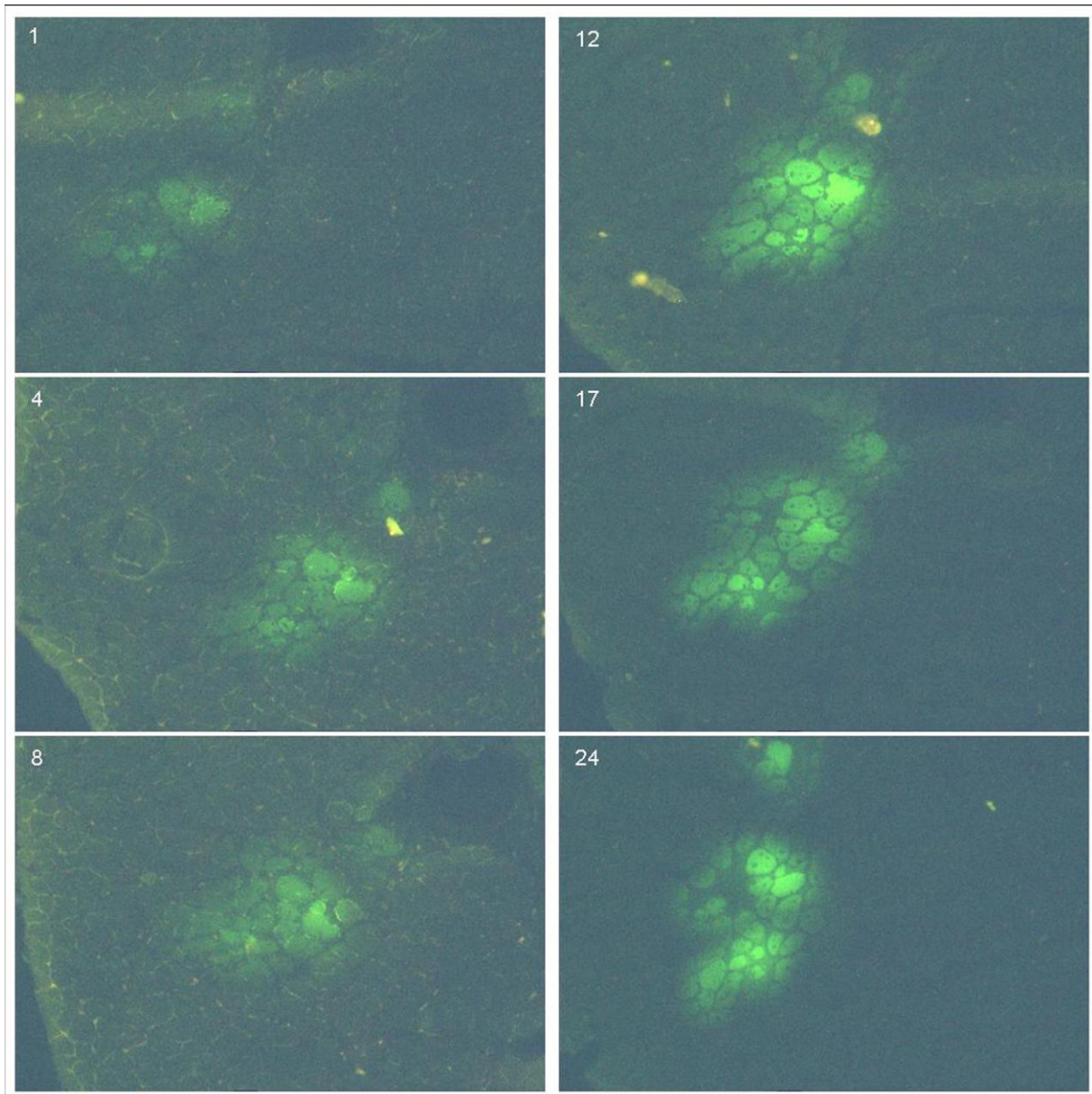


*Figure 5: Representative transversal sections taken consecutively from one segment of regenerating soleus muscle transfected with pEGFP. The order of 1-24 sections is indicated in the*

*upper-left corner. Note that transfection intensity in many fibres changes already after a few sections therefore within a short distance.*

Interestingly besides the above mentioned statistical analysis, transfection efficiency had visible decay already within 240 μm, within a single segment (Fig. 5).

*Staining of neuromuscular endplates on longitudinal sections*

The soleus is a nearly fusiform muscle [37] which suggests that if the transfection is partial along the muscle, the distribution of the transfected nuclei is also uneven in the length of the fibres. However, an average soleus contains up to 3000 fibres in the central segments [25, 96], while in the terminal areas only about 1000 fibres are present (data not shown). Also, at the time of transfection, myotubes might be shorter than later in regeneration [97]. Furthermore it is possible that regenerating myotubes do not fuse with each other but stay divided by myotendous junctions (MTJs) [98]. In order to find out whether the uneven transfection along the muscle was due to shortness of myotubes at the time of the intramuscular plasmid injection, we stained neuromuscular endplates (NME) for acetylcholine esterase (AChE) (Fig. 6). In mammals, each muscle fibre is innervated only by one endplate; therefore, if myotubes did not fuse with each other during regeneration, the position and the number of the endplates would not be the same as in the normal muscle. Since innervation is a prerequisite for the successful regeneration [99] the position of endplates should imply any major change in the average fibre length in the regenerating muscle. The pattern of AChE positive endplates in 11 days regenerated transfected soleus (Fig. 6 C) was similar to that of the normal muscle, except, they were less organized and more diffused, i.e. they followed less even diagonal line on longitudinal sections than in the normal soleus. This diagonal line was a lateral view of the elliptical pattern of NMEs in the muscle mid-belly [71, 100-102]. The number of NME-s in the different segments (Table 2) reveals that NMEs are centrally positioned in regenerating muscles as in the normal soleus. This suggests that fibre length is nearly restored by day 11 of regeneration. Accordingly, matured endplate potentials have been measured by others at this stage in the same type of regeneration of the soleus [99]. Therefore the movement of plasmids and transgenic proteins is probably not limited by fibre length along the 11 days regenerating muscle. However, on longitudinal sections of
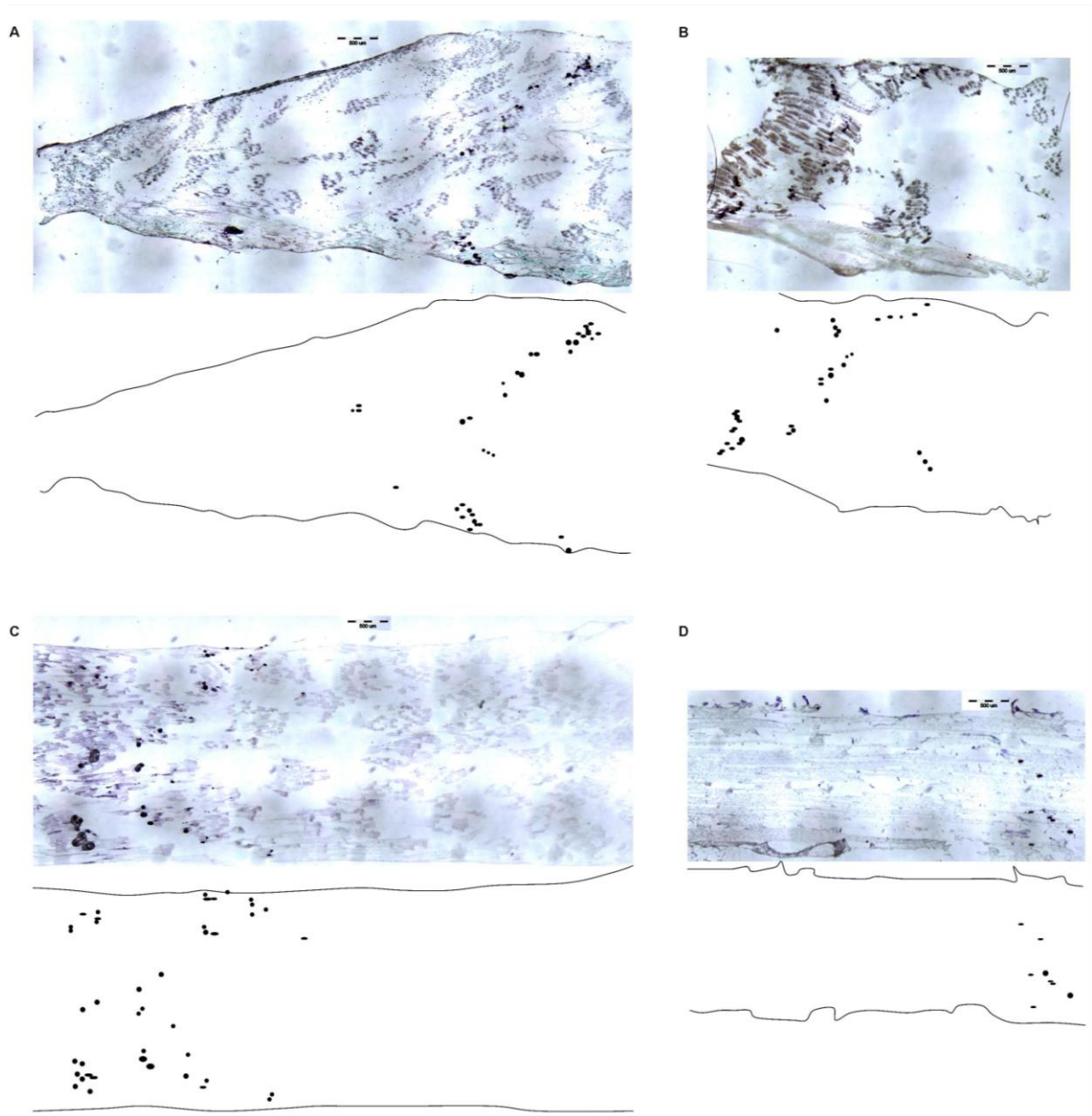
23

*Figure 6: Images of AChE stained longitudinal sections (magnif. 40x) are composed to reconstruct a complete view of the section. A schematic drawing marks the AChE positive endplates under each section. Regenerating soleus on day 5 (A) and day 7 (B), regenerating transfected muscle on day 11 (C) and normal soleus (D). Note that the pattern and distribution of the NMJs are similar in normal and early regenerating muscles, suggesting that this pattern is basically similar later (at more than 7 days) in regeneration (see Table 2).*

5 days regenerating soleus (one day after transfection), the primitive fibres/myotubes were much shorter (Fig. 6) than at day 11 (when the transfection was inspected) or in the

normal muscle [37]. This suggests that the efficient transfection observed in the full length of the 11 days regenerating muscle might be limited by the shortness of myotubes at day 4, at the time of transfection. Therefore anatomical borders like position of transfected nuclei and myotube length at the time of transfection may limit transfection efficiency along the regenerating muscle.

| Muscle | Segments | | | | | |
| ID | 1 | 2 | 3 | 4 | 5 | 6 |
| --- | --- | --- | --- | --- | --- | --- |
| A[1] | 0 | 0 | 66 | 91 | 11 | 5 |
| B[1] | 7 | 5 | 27 | 36 | 67 | 5 |
| C[1] | 4 | 2 | 21 | 55 | 18 | 1 |
| D[1] | 0 | 11 | 38 | 88 | 22 | 0 |
| E[2] | 4 | 0 | 0 | 82 | 37 | 3 |
| F[2] | 0 | 0 | 17 | 16 | 19 | 10 |

**Table 2:** *Number of fibres associated with AChE positive NMJ staining in transfected soleus cross sections at day 11 of regeneration. The highest numbers of NMJ associated fibres are in segments 3-5, at the muscle belly. Normal muscles also exhibit endplates in the central belly, therefore it is likely that transfected regenerating muscles have similar innervation pattern as the normal soleus. [1]muscles transfected with pEFGP or with [2] pDsRed.*

.

*SERCA1b immunohistochemistry on human sections*

Muscle fibres on consecutive post mortem sections stained for SERCA1b or SERCA1 were compared (Fig. 7). Certain fibres stained very strong with anti-SERCA1b antibody while others gave moderate positivity. Many of the intensely stained fibres did not stain for SERCA1 (marked with empty arrows; Fig. 7 A, C) showing that the label with SERCA1b antibody was not specific to the neonatal SERCA1 isoform. On the contrary, immunoblot made from gradient gel loading of the same muscle samples revealed a single protein band in the 110 kDa region, also confirmed by the pan SERCA1 antibody (Fig. 7 E). A similar band was detected when the cDNA of SERCA1b was expressed in

COS-1 cells (Fig. 7 F). This showed that our antibody was specific on immunoblot to human SERCA1b and the two SERCA1 isoforms (having less than 1 % difference in molar mass) were not separated on 8-16 % gradient gel.
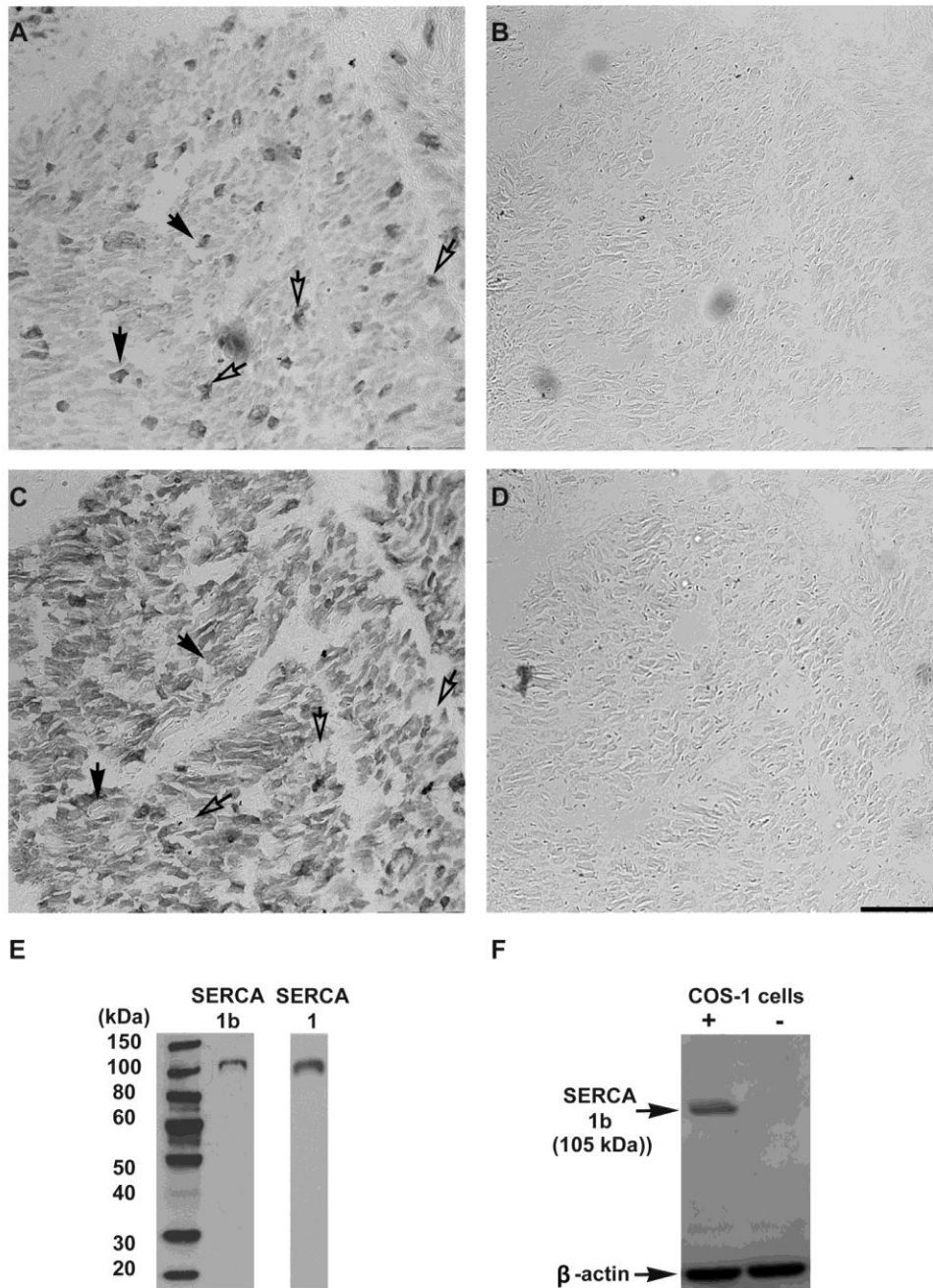


***Figure 7:*** *Representative immunohistochemical staining of post mortem biceps brachii sections of infant III. for SERCA1b (**A**) or SERCA1 (**C**). (**B**) and (**D**) are negative controls without primary antibody. Arrows indicate fibres in similar positions on consecutive slices. Some of the SERCA1b*

*positive fibres (empty arrows) give negative staining with anti-SERCA1 antibody. Since all true-positive SERCA1b fibres should be positive with SERCA1 the staining of those fibres is artefact. Scale bar: 100 µm. (**E**) Immunoblot detection of SERCA1b (left lane) and SERCA1 (right lane) after gradient gel electrophoresis from vastus lateralis of a human foetus. (**F**) Expression of SERCA1b in transfected (left lane: +) and non-transfected (right lane:−) COS-1 cells.*

## SERCA1b Western-blots and RT PCR

The presence of SERCA1b protein has been examined with both SERCA1b specific and panSERCA1 antibodies in human foetal and infant skeletal muscles. SERCA1b was present in leg, arm and gluteal muscles of the two feti (I., II.) and the premature infant (III.), but it was absent in more matured infants (IV., V.) (Fig. 8 A). The SERCA1b positive muscles also had a prominent signal of SERCA1, however some matured infant muscles were positive for SERCA1 and not for SERCA1b indicating the presence of SERCA1a. Similarly the diaphragms (an allotypical skeletal muscle) did not contain
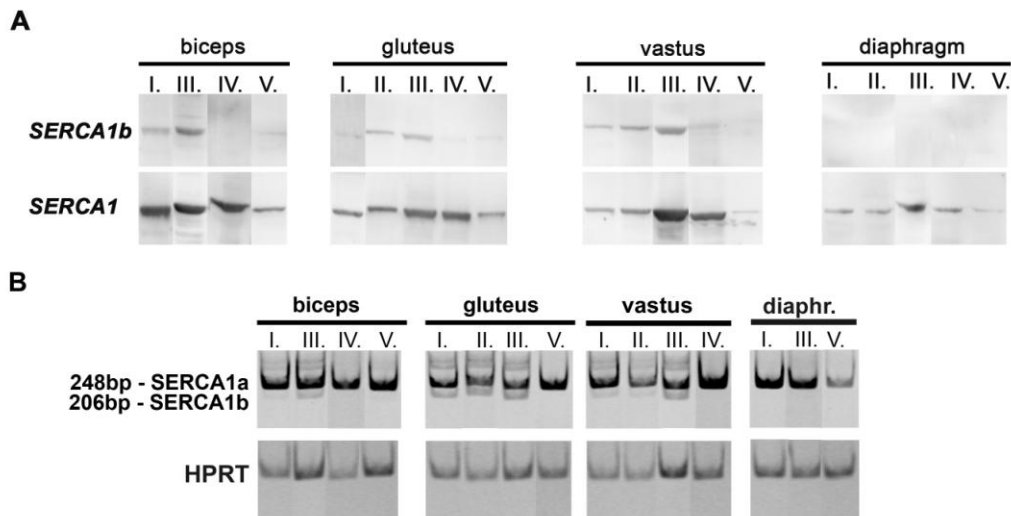


*Figure 8: Immunoblot and PCR detection of SERCA1 isoforms in human muscles. (**A**)Western-blots of membrane fractions from muscles. Loadings are normalized to 5.5 mg fresh weight. Upper row: SERCA1b, lower row: SERCA1. Roman numbers I-V. indicate foeti or infants in the order of age (I.-youngest, V.-oldest). (**B**) PCR analysis for SERCA1a and SERCA1b. SERCA1 was amplified at similar level. Note: none of the muscles expressing SERCA1b RNA missed to translate SERCA1b protein too.*

SERCA1b. To confirm this, increased amounts of loadings from younger and older diaphragm and whole diaphragm lysates (data not shown) were tested and found to be negative for SERCA1b. The gradual loss of SERCA1b paralleled with the relatively strong detection of SERCA1 revealed the increasing amount of SERCA1a in the advanced infant muscles. RT PCR analysis verified the Western-blot results (Fig. 8 D). SERCA1b RNA could only be detected in skeletal muscles of younger objects labelled I-III. Neither of the elder objects nor any of the diaphragms expressed SERCA1b RNA, only the longer SERCA1a transcript. These suggested a transition of SERCA1b and SERCA1a isoforms in neonatal skeletal muscles but not in diaphragms.

We also wanted to estimate the SERCA1b/SERCA1a ratios in the former muscles (Fig. 8) by calculating the SERCA1b and total SERCA1 signal ratios on the same immunoblot. This method shows us that SERCA1b is present in the 5 days regenerating soleus but it is absent in the normal (non-regenerating) soleus (Fig. 9 A) while both muscles are SERCA1 positive [29, 63]. (We must note that the presence of the corresponding SERCA1b and SERCA1a mRNAs was also exclusive in the above developmental stages [29, 63].) We have further tested the SERCA1b/SERCA1 signal ratio for four different loadings from the 5 days regenerating soleus and compared it with the same ratios of loadings of one type of mix of 5 days regenerating and normal soleus on the same membrane. Ratios belonging to different loadings of a certain muscle (or mix of muscles) theoretically should be constant, but are practically different and the mean ratio can be statistically determined by least squares method (see Materials and methods). It is obvious that the SERCA1b/SERCA1 signal ratio for normal soleus (which has no SERCA1b) is significantly lower than that of 5 days regenerating soleus (which has only SERCA1b) (Fig. 9 A). The SERCA1b/SERCA1 ratios for mixed loadings of normal soleus and 5 days regenerating soleus (i.e. 3:1, 2:1 and 1:1) were also significantly lower than that of the 5 days regenerating soleus (Fig. 9 B, C, D). Namely: 1:3 mix: $0.587\pm 0.098$ vs. R: $1.472\pm 0.202$ (p=0.0078); 1:2 mix: $0.774\pm 0.068$ vs. R: $1.485\pm 0.156$ (p=0.0059); 1:1 mix: $1.588\pm 0.355$ vs. R:$3.065\pm 0.409$ (p=0.034) . This shows that the SERCA1a content can be detected next to SERCA1b in this way. This type of analysis can reveal the presence of SERCA1a in at least a 1:1 mix of SERCA1a and SERCA1b. We assume that a lower SERCA1a ratio may not result in significant difference from the pure SERCA1b because of the limited quantitative nature of the immunoblot method.
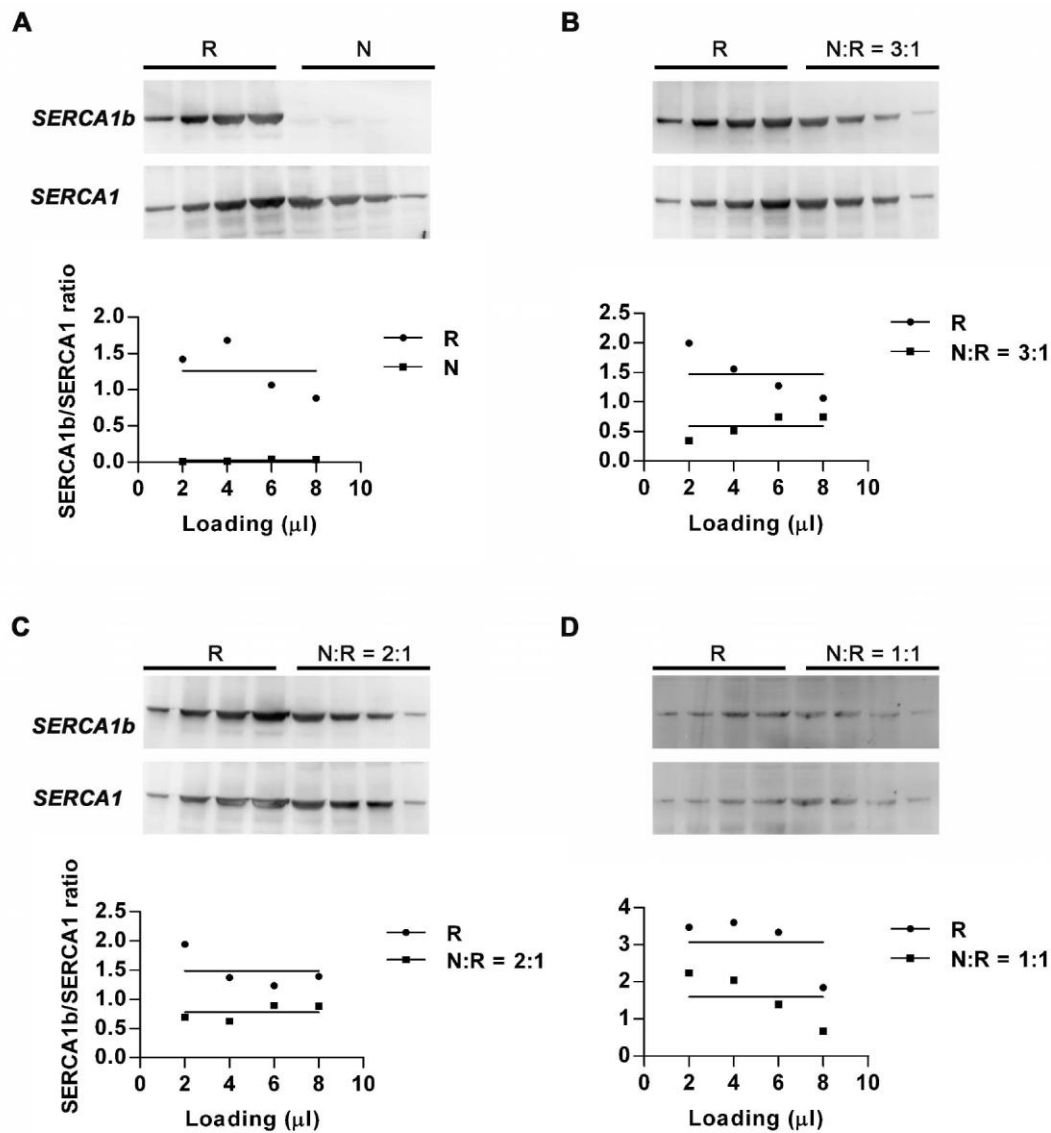
***Figure 9:*** *Comparison of SERCA1b/SERCA1 signal ratios in normal and 5 days regenerating rat soleus muscles and in their different mixtures. Panels: The first 4 lanes on each membrane show loading series of regenerating soleus membrane fractions (2-4-6-8 μl loadings), the second 4 lanes are the same loadings in reciprocal order (**A**) from normal soleus or mixtures ((**B**) 3:1, (**C**) 2:1, (**D**) 1:1 of normal:regenerating muscles). Diagrams on each panel show SERCA1b/SERCA1 signal ratios of different loadings. Lines represent the SERCA1b/SERCA1 signal ratio of the chosen muscle calculated with statistical methods (see Materials and methods). Note: There is practically only SERCA1a signal in normal soleus muscle and only SERCA1b in the 5 days regenerating soleus (**A**). The SERCA1b/SERCA1 signal ratios are significantly higher in regenerating soleus than in mixtures of normal and 5 days regenerating soleus extracts (**B-D**). This experiment indicates that the presence of SERCA1a can be shown at least down to 50% of*

*total SERCA1 by the SERCA1b/SERCA1 signal ratio on immunoblots. R: regenerating soleus, N: normal soleus; level of significance p< 0,05.*

We used the above described method to obtain more information about the SERCA1a content of those perinatal human muscles which contained SERCA1b (Fig. 8 A). Serial loadings of human samples were run parallel with loading series of SERCA1b containing regenerating soleus muscle on the same gels (Fig. 10). SERCA1b/SERCA1 signal ratios were significantly less in all human samples than in regenerating muscles (Fig. 10 A-C) showing that a significant portion of SERCA1a is also present (B: 0.234± 0.044 vs. R:
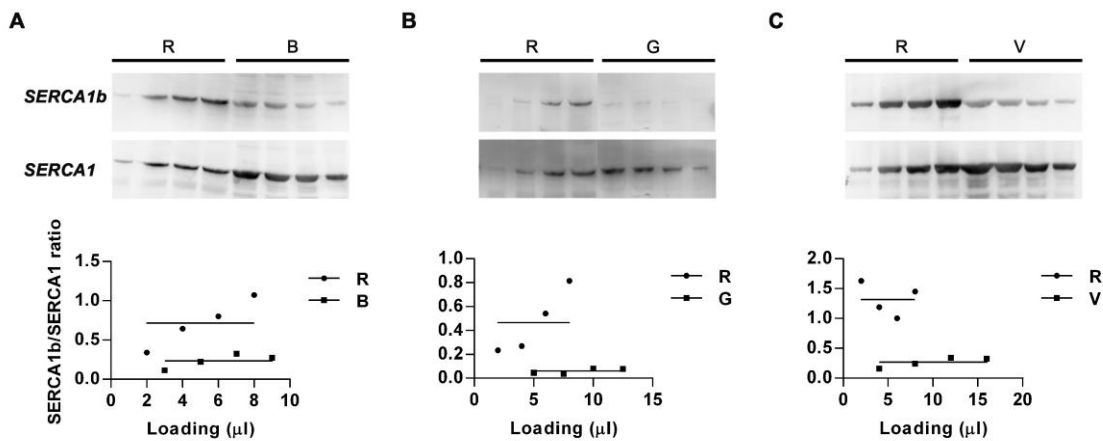


***Figure10:*** *SERCA1b/SERCA1 signal ratios in different human muscles compared to the ratio in regenerating soleus. Panels: The first 4 lanes on each membrane show the loading series of regenerating soleus (2-4-6-8 µl); the second 4 lanes are loading series of different human muscles in reciprocal order (loadings were adjusted to linear detection range). (**A**) biceps brachii of infant III. (loadings: 9-7-5-3 µl; highest loading refers to 6 mg fresh weight); (**B**) gluteus maximus of fetus II. (loadings: 12.5-10-7.5-5 µl; highest loading refers to 9 mg fresh weight); (**C**) vastus lateralis of infant III. (loadings: 16-12-8-4 µl; highest loading refers to 8 mg fresh weight). Diagrams on each panel show SERCA1b/SERCA1 signal ratios according to different loadings. Lines represent the SERCA1b/SERCA1 signal ratio of the chosen muscle calculated with statistical methods (see Materials and methods). Note: Ratio of each investigated human muscle is significantly under that of the 5 days regenerating soleus. This indicates that each of them expresses both SERCA1a and SERCA1b. Particularly, in the gluteus maximus of fetus II, whose SERCA1b/SERCA1 signal ratio is only 12,8% of that of regenerating soleus, has probably the*

$0.714\pm 0.153$ (p=0.0238); G: $0.059\pm 0.010$ vs. R: $0.464\pm 0.135$ (p=0.0246), V: $0.269\pm 0.041$ vs. R: $1.317\pm 0.138$ (p=0.0004)). Comparing these experiments with the ratios in muscle mixes tested on Fig. 9, the biceps brachii of object III., gluteus maximus muscle of object II. and vastus lateralis of object III. could have contained SERCA1a higher than 50% of total SERCA1 protein therefore although SERCA1b was present, SERCA1a was the dominant isoform in these muscles.

Western-blots of healthy human adult muscle homogenates, DM1 and DMD muscles (DMD children around the age of 10) (Fig. 11) did not reveal the presence of SERCA1b in contrast to the investigated DM2 samples (adults around the age of 40).
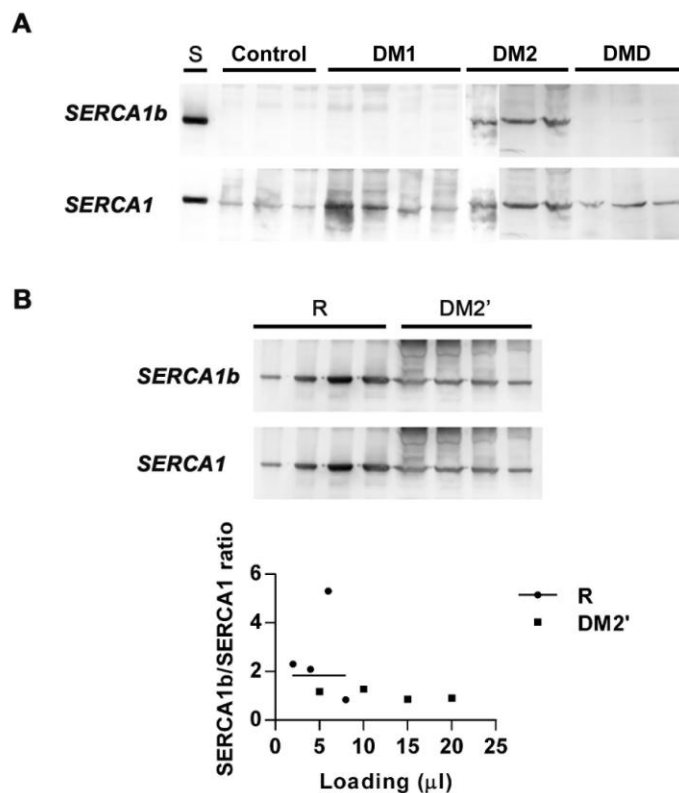


*Figure 11: SERCA1b and SERCA1 expression in normal, and diseased muscle (DM1, DM2 and DMD). (A) 6 μl rat regenerating soleus SR homogenate serves as positive control in the first lane, loading of human samples was normalized to 100 μg total protein. Note: Only DM2 muscles contained SERCA1b despite the much higher age compared to DMD patients (B) First 4 lanes show the loading series of regenerating soleus (2-4-6-8 μl); the second 4 lanes are loading series from one of the DM2 muscles (DM2') in decreasing order (20-15-10-5 μl; highest loading refers to: 100 μg total protein). SERCA1b /SERCA1 signal ratios of regenerating soleus and DM2' muscles do not differ significantly, therefore only one curve is fitted. This means that the proportion of SERCA1b is similar in these muscles. S: regenerating rat soleus, DM1:*

*myotonic dystrophy type 1, DM2: myotonic dystrophy type 2, DMD: Duchenne muscular dystrophy (samples referred as Italian and Belgian muscle biopsies). Level of significance: p< 0,05.*

However all four groups were SERCA1 positive therefore SERCA1b in DM2 patients might have a share in SERCA1. The SERCA1b/SERCA1 signal ratio of one of the SERCA1b positive DM2 muscles was compared with that of pure regenerating soleus (Fig. 11 B). There was no significant difference between the ratios of the DM2 muscle and the 5 days regenerating soleus (DM2: 1.050±0.101 vs. R: 2.634±0.947 (p=0.1473)), indicating that SERCA1 in the DM2 muscle is predominantly if not entirely SERCA1b.

## DISCUSSION:

### Transfection efficiency along the regenerating muscle

Transversal sections taken systematically along the soleus muscle showed that the number of transfected fibres was higher in the central parts and decreased toward the proximal and distal ends; this finding was independent of the used reporter genes. To monitor transfection along the fibres, we divided the fusiform soleus muscle in length into six equal segments (4-5 mm, 1/6 of muscle length). EGFP and DsRed expressions in the fibres declined already along a single segment. Such an uneven transgene expression has been reported previously along the fibres of mouse rectus femoris [35]. The distal and proximal fibre ends showed pronounced β-galactosidase expression 3-6 hours after transfection which turned out to be somehow more evenly distributed along the fibres at 4 days after plasmid treatment. In another study, the transfected β-galactosidase exhibited segmental differences within the fibres of regenerating rat soleus muscles on serially cross and longitudinal sections [34]. This latter finding has not been supported by the whole-mount analysis of EDL muscles in mice, where the GFP occupied the whole fibre [103] and a similar observation was made after single fibre transfection [36].

To interpret the declining expression levels along the fibres, we should consider that plasmids are not homogenously distributed along the entire muscle after being injected.

Doh et al. [35] hypothesized that DNA could accumulate in "pockets" which could be responsible for the varying expression pattern. In our opinion, such pockets could be even more frequent in regenerating than in normal muscles, which often contain i.e. split fibres [104]. In addition, if we consider that 95% of the plasmids is degraded in the first 6 hours in the interstitial space [105], the chance of long-term diffusion is indeed extremely low. Plasmids have to be incorporated next to the site of injection and this happens in case of only a few nuclei [36]. The nuclear resident plasmids express the transgene in the vicinity called myonuclear domain. Since fibres in mice muscles are smaller than in rat muscles, the transgene concentration can be equalized more efficiently in mice than in rat muscles [36, 103]. The distance of DNA-containing "pockets" from transfectable nuclei and the diffusion-limits of the expressed gene products seem to be plausible explanations for the uneven transgene distribution along the fibres.

The other explanation is the limited ic. transport of the transfected plasmids. One reason for this is that the myotubes were shorter at the time of transfection than at the time of monitoring EGFP expression. Plasmids injected to the central part of the regenerating soleus had little chance to get to muscle ends because the myotubes/young fibres were much shorter than the whole muscle length [97]. Later, when the young fibres fused with each other the transfected nuclei still remained on spot [106-110]. Other literature also describes that young myotubes are divided by myotendonal junctions in regenerating muscle and later develop into longer fibres [98].

Since each fibre has one innervation in mammals [111], we used NMJs to test the fusion of myotubes as an indirect control of fibre length. If the myotubes did not fuse by day 11 of regeneration (when the transfection was inspected) the number of NMJs would increase at muscle ends. On the contrary, if the myotubes managed to fuse, the NMJs should still be at the mid-belly like in the normal soleus [100]. Our results showed that the NMJs were approximately in the same position in the regenerating and normal muscles on longitudinal and cross sections. The innervation of most fibres is completed by day 7 of regeneration [99, 112], after this it is less likely that the fibres are interrupted by myotendonal junctions (MTJs). We analysed regenerating muscles at day 5, (one day after transfection) and day 11 (when the transfection was inspected). We found that fibre length was relatively short on day 5 and it appeared longer at day 11, almost as long as in the untreated soleus; though fibre CSAs are significantly behind that of normal muscles.

Therefore, as a consequence, we can say that the uneven distribution of transfection in the regenerating muscle is probably due to the fixed position of transfected nuclei and to the limited diffusion of the expressed transgenic proteins. The regional changing of transfection means that the efficiency cannot be estimated accurately from the most transfected central part of the muscle. Therefore, growth stimulations in the entire regenerating soleus that were achieved by transfecting only a few fibres with signal pathway inhibitors [24, 25] must have been initiated from a smaller part of the muscle than it seemed previously.

*SERCA1b in not diseased human muscles*

The potent regulatory role of SERCA1b in rat signalisation processes during muscle regeneration was already suspected. First results of SERCA1b immunohistochemistry on human fetal/neonatal sections also suggested that this protein was also expressed during early human muscle development. Finally we have found that only the premature infant and foeti contained SERCA1b in their skeletal muscle. This information was based on clear immunoblot signals from microsomal membrane protein homogenates since immunohistochemistry for SERCA1 revealed that the signals obtained by anti-SERCA1b antibody were false positive on post mortem muscle sections. The reason for the false positivity might be that according to the UniProt database the octapeptide tail of SERCA1b is present within the peptide chain of several other muscle proteins and these after auto proteolysis of post mortem samples stored at 4-8°C for several days could result in unspecific staining. The dominating SERCA isoform detected during early development of rodents is SERCA1b, independent of muscle type [63]. In human, according to immunoblot analysis SERCA1b was present exclusively during pregnancy (i.e. in two intrauterine exits and one premature infant with corrected gestational age of 32 weeks). These data confirm relevance of the question: why is SERCA1b expressed only in early development? Foetal movements are limited in the womb and SERCA1b mRNA expression was connected with muscle activity, i.e. passive stretch (a condition of overload) and denervation [63, 113]. However the increase of SERCA1b mRNA level was paralleled with that of the protein only in immature fibres and not in the above mentioned adult conditions.

In order to gain more information about the SERCA1a content of human muscles that also expressed SERCA1b, experiments were designed with normal and 5 days regenerating rat soleus. The normal soleus contained practically only SERCA1a and only SERCA1b was present in the 5 days regenerating soleus. These two muscles provided a negative and positive source of SERCA1b while both were positive for SERCA1. We assumed that mixes of different ratios of the two muscles will give a scale to estimate the SERCA1a proportion within the total SERCA1 pool. The SERCA1b/SERCA1 signal ratios estimated from loading series of certain mixtures of SERCA1a and SERCA1b enabled to verify the presence of SERCA1a only if the ratio to SERCA1a was above 50%. By this method we demonstrated that SERCA1a was the predominant isoform even in those foetal and neonatal muscles that also contained SERCA1b. We suppose that if SERCA1b were dominant in early foetal muscles there might be a transition from SERCA1b to SERCA1a expression while these muscles are differentiating towards the matured phenotype. The dominant level of SERCA1a in neonatal muscles and the absence of SERCA1b even in the foetal diaphragms highlight the difference between humans and rodents during the time course of muscle development. However, it cannot be excluded that SERCA1b is the dominant SERCA1 isoform in younger human foeti like it was implied in a preliminary experiment [63]. We must emphasise that our samples were muscle biopsies containing no brown adipose tissue (BAT) according to their localisation. BAT is important for thermoregulation in foeti and mature infants and expresses SERCA1 that is directly involved in thermogenesis. Despite of its different features from muscle SERCA1, the BAT SERCA1 has not been cloned and sequenced yet [59-61, 114]. Therefore it would be of great interest whether BAT and skeletal muscle share a common origin also in respect of SERCA1b. It is worth to note that there are alternative SERCA1 isoforms in poikilothermic animals with polar C-terminal sequence like that in SERCA1b of rat and human. These transcripts are present in the heather organ of fish and brought in connection with cold adaptation in frog [115, 116].

According to our PCR results SERCA1b − SERCA1a protein ratios are in accordance with their mRNA ratios. This suggests that SERCA1b protein expression in young humans is also regulated at the splicing level. The alternative splicing of exon 22 (the one spliced out in SERCA1b but not in SERCA1a) is directly regulated by muscleblind-like proteins (MBNL). MBLN-1 has been proven to have 5 binding motifs on SERCA1 pre-

mRNA, downstream from exon 22 on intron 22. In presence of MBNL-1, -2 and -3 exon 22 remains in the mRNA and SERCA1a is translated [86]. Regulation of MBNL proteins is possible via its protein kinase C phosphorylation sites (reviewed by [117]). All these have relevance in the pathomechanism of DM and have already been targeted in research for therapy [118]. There is a CUG triplet expansion in the myotonic dystrophy protein kinase (DMPK) mRNA of patients suffering from DM. Since MBNL molecules are needed to regulate alternative splicing of certain genes (like SERCA1, SERCA2, muscle-specific insulin receptor [86, 119, 120]) and also have affinity for binding CUG triplets, the abundance of MBLN proteins decreases in case of CUG expansion and muscle fibres might undergo aberrant spicing.

*SERCA1b protein in diseased human muscles*

We have investigated two illnesses out of those that were brought in connection with the muscle specific SERCA1. One of them was the dystrophia myotonica type 2 (DM2) where splicing of several mRNAs is disturbed and SERCA1b mRNA is expressed at even higher level than in the similar disease, the type 1 myotonic dystrophy (DM1) [68, 85-88]. However, unlike in DM1, many small fibres with nuclear clumps, and rare connective fibrosis are found in DM2 indicating the presence of regeneration [121], a condition found to be a requisite of SERCA1b protein expression in rodents. In accordance, we found that the SERCA1b protein is present in DM2, which seemed to correlate with its high mRNA level [121] and represented the dominant fraction of SERCA1 isoforms in the investigated (quadriceps) muscle.

The other investigated muscle disease, DMD is a typical progressive degenerative-regenerative disorder, with strong regeneration process that is exhausting by time. However there are certain muscles which are spared in these patients (i.e. laryngeal, extraocular and toe muscles). Spared muscles exhibit an increase in SERCA1 expression [78]. This implies that analysing $Ca^{2+}$ handling proteins in affected muscles might be important for developing possible treatment. We could not detect SERCA1b in TA muscle affected by the disease in DMD patients, therefore the SERCA1 signal obtained on immunoblot originated solely from SERCA1a protein. Recent results show that upregulation of the Orai1-mediated SOCE pathway may contribute to altered $Ca^{2+}$-homeostasis in mdx mice, consequently grade of SR $Ca^{2+}$-filling is higher. Parallel with

this SERCA1 expression is reduced which is hypothesized to be a compensatory response to the filled SR stores [122]. Even if this downregulation also occurred in human, it is a question why the remaining SERCA1 isoform SERCA1a is and not SERCA1b in spite the regenerative background of this disease? One explanation might be that DMD patients received corticosteroid therapy, and corticosteroids are known to decrease SERCA1 transcript level [123]. Another, more likely possibility is that children in DMD at ages 7-12 have already exhausted regenerative capacity thereby lacking the cellular background for SERCA1b expression.

Skeletal muscle regeneration and repair after muscle injury recapitulates the main steps of normal muscle development. There is however a huge difference, since normal muscles grow along MTJs, at fibre ends [124], while injured or diseased muscle has to correct itself by satellite cells even in the middle of the fibre (reviewed by [110]). The formation of sarcomer structure and SR maturation play essential roles during early muscle development. Recent data show that the former ones are closely related to the appropriate organization of myoblasts and the differentiation of myotubes [125]. Fusion of myoblasts to myotubes is followed by the addition of further nuclei to the performed myotubes/multinucleated fibres which is stimulated by $PGF_{2\alpha}$ [126] and the regulation of secreted IL-4. IL-4 is induced by NFATc2, which also allows increment of fibre CSA [48, 108]. Growth is also in strong relation with structural differentiation. Long duration $Ca^{2+}$-transients of early development are gradually replaced by RyR-dependent short duration transients that enable sarcomere assembly [127]. This process is also accompanied by T-tubule formation. First structural components of T-tubules dock to the SR in a longitudinal position, that is followed by RyR insertion and positioning of the complex within the sarcomere that allows the transverse orientation of the T-tubule [128]. Striated pattern of SERCA associated to Z-discs was brought in connection with appearance of ank1.5 protein clusters along M bands [129]. Why it is beneficial to express SERCA1b proteins in early muscle development, instead of SERCA1a, is however still an open question. Previous results have also shown that SERCA1 could have impact on morphologic organisation of SR from the ER in cultured fibroblasts [130]. The prerequisite for this is a SERCA1 concentration that reaches levels like that in skeletal muscle. This event is linked to SERCA1 protein structure itself, since SR-like tubular membrane bundles are formed with SERCA1 mutant even without catalytic

activity. This could further underline the impact of SERCA1 during myogenesis. In one or other way influence on signal transduction would also be logic. It is however not known in what manner, by long-term alteration of intracellular $Ca^{2+}$-concentrations [131], or by specific protein-protein interactions may be enabled through the C-terminal octapeptide.

## NOVEL RESULTS OF THE THESIS

- With a whole muscle analysis we have shown that the basic transfection technique, the naked plasmid injection results in lower transfection efficiency than it has been previously thought.
- We demonstrated that the SERCA1b protein is expressed during early muscle development in human and it is replaced by SERCA1a in the first months of life.
- We have developed a novel method for detection of SERCA1b or SERCA1a dominance at the protein level
- SERCA1b is abundantly expressed in muscles of DM2 patients even at 40 years age unlike in the muscles of DM1 patients and healthy adults.

## SUMMARY

This work studied the neonatal sarcoplasmic/endoplasmic reticulum $Ca^{2+}$-ATPase (SERCA1b) from two different aspects. The first aspect was the transfection efficiency of intramuscular plasmid injection delivering SERCA1b RNAi that resulted in a significant increase of whole muscle mass and cross sectional area in the regenerating soleus muscle of rat. As the method had low transfection efficiency in the injection area and an unknown distribution in the rest of the muscle, our aim was to monitor transfection systematically in longitudinal and transversal directions in the rat soleus. Transfection with EGFP and DsRed plasmids was spatially restricted along the fibres revealing a much lower efficiency than it was previously assumed. Since transfection of the SERCA1b RNAi expressing plasmid even at such low efficiency resulted in significant growth stimulation in the whole regenerating soleus, the result highlights the importance of SERCA1b expression in developing muscle. The second aspect of our study was to investigate the presence of SERCA1b in human developing skeletal muscles. We developed a method using antibody selectively recognizing SERCA1b but not SERCA1a in combination with pan SERCA1 antibody that recognised both. We found that SERCA1b protein and RNA are disappearing with age in muscles of human feti and newborns. In contrast, diaphragms did not express SERCA1b in foetal or infant age. At least three diseases were brought in connection with altered SERCA1 expression: the type 1 and type 2 myotonic dystrophies (DM1, DM2) and the Duchenne muscular dystrophy (DMD). Among these only DM2 expressed SERCA1b as the major SERCA1 isoform in the investigated muscle, the two other diseases showed only SERCA1a.

In conclusion, the detected low transfection efficiency of RNAi further underlines the importance of SERCA1b in muscle regeneration and development. According to its expression this pump could have a similar role in human as in rats since it is also expressed in muscles at the end of pregnancy and in early neonatal ages. However the time scale of diaphragmatic and birth related expression is different in the two species. From the investigated human diseases only DM2 exhibited SERCA1b expression in muscles which is a new data for the pathomechanism of this condition.

## ACKNOWLEDGEMENTS

I would like to thank Dr. Ernő Zádor for his work as my supervisor and for offering Fig. 5 and Fig. 7 F for this work, Prof. László Dux for allowing me to work in his department and Dr. Csaba Bereczky for his later support as my present chief.

I would also like to thank Dr. Luca Mendler for her methodological advices; Dr. Kitti Brinyiczki for taking post mortem human samples and Dr. László Kaiser for his support; Károly Hancsák for advices on statistics, Dr. Lajos Pintér and Lajos Haracska for the possibility to use the Typhoon scanner; Dr. Philip van Damme, Dr. Nathalie. Goemans, Dr. Gaetamo Vattemi for biopsies of diseased muscles.

**REFERENCES:**

1. Miller, G., et al., *Expression of factor VII by muscle cells in vitro and in vivo following direct gene transfer: modelling gene therapy for haemophilia.* Gene Ther, 1995. **2**: p. 736-742.

2. Arruda, V.R., et al., *Peripheral transvenular delivery of adeno-associated viral vectors to skeletal muscle as a novel therapy for hemophilia B.* Blood, 2010. **115**: p. 4678-4688

3. Tripathy, S.K., et al., *Stable delivery of physiologic levels of recombinant erythropoietin to the systemic circulation by intramuscular injection of replication-defective adenovirus.* Proc Natl Acad Sci U S A, 1994. **91**: p. 11557-11561.

4. Naffakh, N., et al., *Long-term secretion of therapeutic proteins from genetically modified skeletal muscles.* Hum Gene Ther, 1996. **7**: p. 11-21.

5. Czibik, G., et al., *Gene therapy with hypoxia-inducible factor 1 alpha in skeletal muscle is cardioprotective in vivo.* Life Sci, 2011. **88**: p. 543-550.

6. Bilbija, D., et al., *Protecting the heart through delivering DNA encoding for heme oxygenase-1 into skeletal muscle.* Life Sci, 2012. **91**: p. 828-836.

7. Isaka, Y., et al., *Gene therapy by skeletal muscle expression of decorin prevents fibrotic disease in rat kidney.* Nat Med, 1996. **2**: p. 418-423.

8. Montgomery, D.L., et al., *DNA vaccines.* Pharmacol Ther, 1997. **74**: p. 195-205.

9. Safwat, Y., et al., *Modulation of skeletal muscle performance and SERCA by exercise and adiponectin gene therapy in insulin-resistant rat.* DNA Cell Biol, 2013. **32**: p. 378-385.

10. Piccioni, A., et al., *Sonic hedgehog therapy in a mouse model of age-associated impairment of skeletal muscle regeneration.* J Gerontol A Biol Sci Med Sci, 2014. **69**: p. 245-252.

11. Witzenbichler, B., et al., *Intramuscular gene transfer of fibroblast growth factor-1 using improved pCOR plasmid design stimulates collateral formation in a rabbit ischemic hindlimb model.* J Mol Med (Berl), 2006. **84**: p. 491-502.

12. Baumgartner, I., et al., *Local gene transfer and expression following intramuscular administration of FGF-1 plasmid DNA in patients with critical limb ischemia.* Mol Ther, 2009. **17**: p. 914-921.

13. Odom, G.L., P. Gregorevic, and J.S. Chamberlain, *Viral-mediated gene therapy for the muscular dystrophies: successes, limitations and recent advances.* Biochim Biophys Acta, 2007. **1772**: p. 243-262.

14. Jafari, M., et al., *Nonviral approach for targeted nucleic acid delivery.* Curr Med Chem, 2012. **19**: p. 197-208.

15. Vitadello, M., et al., *Gene transfer in regenerating muscle.* Hum Gene Ther, 1994. **5**: p. 11-18.

16. Mir, L.M., et al., *High-efficiency gene transfer into skeletal muscle mediated by electric pulses.* Proc Natl Acad Sci U S A, 1999. **96**: p. 4262-4267.

17. Molnar, M.J., et al., *Factors influencing the efficacy, longevity, and safety of electroporation-assisted plasmid-based gene transfer into mouse muscles.* Mol Ther, 2004. **10**: p. 447-455.

18. Schertzer, J.D., D.R. Plant, and G.S. Lynch, *Optimizing plasmid-based gene transfer for investigating skeletal muscle structure and function.* Mol Ther, 2006. **13**: p. 795-803.

19. Lu, Q.L., et al., *Microbubble ultrasound improves the efficiency of gene transduction in skeletal muscle in vivo with reduced tissue damage.* Gene Ther, 2003. **10**: p. 396-405.

20. Lemieux, P., et al., *A combination of poloxamers increases gene expression of plasmid DNA in skeletal muscle.* Gene Ther, 2000. **7**: p. 986-991.

21. Chang, C.W., et al., *Non-ionic amphiphilic biodegradable PEG-PLGA-PEG copolymer enhances gene delivery efficiency in rat skeletal muscle.* J Control Release, 2007. **118**: p. 245-253.

22. Yang, N.S., et al., *In vivo and in vitro gene transfer to mammalian somatic cells by particle bombardment.* Proc Natl Acad Sci U S A, 1990. **87**: p. 9568-9572.

23. Zhang, G., et al., *Efficient expression of naked dna delivered intraarterially to limb muscles of nonhuman primates.* Hum Gene Ther, 2001. **12**: p. 427-438.

24. Zador, E., *dnRas stimulates autocrine-paracrine growth of regenerating muscle via calcineurin-NFAT-IL-4 pathway.* Biochem Biophys Res Commun, 2008. **375**: p. 265-270.

25. Zador, E., G. Owsianik, and F. Wuytack, *Silencing SERCA1b in a few fibers stimulates growth in the entire regenerating soleus muscle.* Histochem Cell Biol, 2011. **135**: p. 11-20.

26. Harris, J.B., M.A. Johnson, and E. Karlsson, *Pathological responses of rat skeletal muscle to a single subcutaneous injection of a toxin isolated from the venom of the Australian tiger snake, Notechis scutatus scutatus.* Clin Exp Pharmacol Physiol, 1975. **2**: p. 383-404.

27. Harris, J.B., E. Karlsson, and S. Thesleff, *Effects of an isolated toxin from Australian Tiger snake (Notechis scutatus scutatus) venom at the mammalian neuromuscular junction.* Brit J Pharmacol, 1973. **47**: p. 141-146.

28. Whalen, R.G., et al., *Expression of myosin isoforms during notexin-induced regeneration of rat soleus muscles.* Dev Biol, 1990. **141**: p. 24-40.

29. Zador, E., et al., *Changes in mRNA levels of the sarcoplasmic/endoplasmic-reticulum Ca(2+)-ATPase isoforms in the rat soleus muscle regenerating from notexin-induced necrosis.* Biochem J, 1996. **320**: p. 107-113.

30. Harris, J.B., et al., *Muscle fibre breakdown in venom-induced muscle degeneration.* J Anat, 2003. **202**: p. 363-372.

31. Klein-Ogus, C. and J.B. Harris, *Preliminary observations of satellite cells in undamaged fibres of the rat soleus muscle assaulted by a snake-venom toxin.* Cell Tissue Res, 1983. **230**: p. 671-676.

32. Harris, J.B., *Myotoxic phospholipases A2 and the regeneration of skeletal muscles.* Toxicon, 2003. **42**: p. 933-945.

33. Mir, L.M., et al., *High-efficiency gene transfer into skeletal muscle mediated by electric pulses.* Proc Natl Acad Sci U S A, 1999. **96**: p. 4262-4267.

34. Vitadello, M., et al., *Gene transfer in regenerating muscle.* Hum Gene Ther, 1994. **5**: p. 11-18.

35. Doh, S.G., et al., *Spatial-temporal patterns of gene expression in mouse skeletal muscle after injection of lacZ plasmid DNA.* Gene Ther, 1997. **4**: p. 648-663.

36. Utvik, J.K., A. Nja, and K. Gundersen, *DNA injection into single cells of intact mice.* Hum Gene Ther, 1999. **10**: p. 291-300.

37. Stickland, N., *The arrangement of muscle fibers and tendons in two muscles used for growth studies.* J Anat, 1983. **136**: p. 175-179.

38. Wang, Z.M., et al., *Residual sarcoplasmic reticulum Ca2+ concentration after Ca2+ release in skeletal myofibers from young adult and old mice.* Pflugers Arch, 2012. **463**: p. 615-624.

39. Rosenberg, P., et al., *TRPC3 channels confer cellular memory of recent neuromuscular activity.* Proc Natl Acad Sci U S A, 2004. **101**: p. 9387-9392.

40. Calabria, E., et al., *NFAT isoforms control activity-dependent muscle fiber type specification.* Proc Natl Acad Sci U S A, 2009. **106**: p. 13335-13340.

41. Varnai, P., L. Hunyady, and T. Balla, *STIM and Orai: the long-awaited constituents of store-operated calcium entry.* Trends Pharmacol Sci, 2009. **30**: p. 118-128.

42. Stiber, J.A. and P.B. Rosenberg, *The role of store-operated calcium influx in skeletal muscle signaling.* Cell Calcium, 2011. **49**: p. 341-349.

43. Cahalan, M.D., *STIMulating store-operated Ca(2+) entry.* Nat Cell Biol, 2009. **11**: p. 669-677.

44. Zhang, S., et al., *STIM1 is a Ca2+ sensor that activates CRAC channels and migrates from the Ca2+ store to the plasma membrane.* Nature, 2005. **437**: p. 902-905.

45. Liou, J., et al., *STIM is a Ca2+ sensor essential for Ca2+-store-depletion-triggered Ca2+ influx.* Curr Biol, 2005. **15**: p. 1235-1241.

46. Liou, J., et al., *Live-cell imaging reveals sequential oligomerization and local plasma membrane targeting of stromal interaction molecule 1 after Ca2+ store depletion.* Proc Natl Acad Sci U S A, 2007. **104**: p. 9301-9306.

47. Stiber, J., et al., *STIM1 signalling controls store-operated calcium entry required for development and contractile function in skeletal muscle.* Nat Cell Biol, 2008. **10**: p. 688-697.

48. Horsley, V., et al., *IL-4 acts as a myoblast recruitment factor during mammalian muscle growth.* Cell, 2003. **113**: p. 483-494.

49. Seth, M., et al., *Dynamic regulation of sarcoplasmic reticulum Ca(2+) stores by stromal interaction molecule 1 and sarcolipin during muscle differentiation.* Dev Dyn, 2012. **241**: p. 639-647.

50. Tavi, P. and H. Westerblad, *The role of in vivo Ca(2)(+) signals acting on Ca(2)(+)-calmodulin-dependent proteins for skeletal muscle plasticity.* J Physiol, 2011. **589**: p. 5021-5031.

51. Michalak, M., et al., *Calreticulin, a multi-process calcium-buffering chaperone of the endoplasmic reticulum.* Biochem J, 2009. **417**: p. 651-666.

52. Canato, M., et al., *Massive alterations of sarcoplasmic reticulum free calcium in skeletal muscle fibers lacking calsequestrin revealed by a genetically encoded probe.* Proc Natl Acad Sci U S A, 2010. **107**: p. 22326-22331.

53. Yoshida, M., et al., *Impaired Ca2+ store functions in skeletal and cardiac muscle cells from sarcalumenin-deficient mice.* J Biol Chem, 2005. **280**: p. 3500-3506.

54. Brandl, C.J., et al., *Adult forms of the Ca2+ATPase of sarcoplasmic reticulum. Expression in developing skeletal muscle.* J Biol Chem, 1987. **262**: p. 3768-3774.

55. Wuytack, F., L. Raeymaekers, and L. Missiaen, *Molecular physiology of the SERCA and SPCA pumps.* Cell Calcium, 2002. **32**: p. 279-305.

56. Burk, S.E., et al., *cDNA cloning, functional expression, and mRNA tissue distribution of a third organellar Ca2+ pump.* J Biol Chem, 1989. **264**: p. 18561-18568.

57. Stephenson, G.M., *Hybrid skeletal muscle fibres: a rare or common phenomenon?* Clin Exp Pharmacol Physiol, 2001. **28**: p. 692-702.

58. Chami, M., et al., *SERCA1 truncated proteins unable to pump calcium reduce the endoplasmic reticulum calcium concentration and induce apoptosis.* J Cell Biol, 2001. **153**: p. 1301-1314.

59. de Meis, L., *Brown adipose tissue Ca2+-ATPase: uncoupled ATP hydrolysis and thermogenic activity.* J Biol Chem, 2003. **278**: p. 41856-41861.

60. de Meis, L., et al., *Identification of a Ca2+-ATPase in brown adipose tissue mitochondria: regulation of thermogenesis by ATP and Ca2+.* J Biol Chem, 2006. **281**: p. 16384-16390.

61. de Meis, L., et al., *Fusion of the endoplasmic reticulum and mitochondrial outer membrane in rats brown adipose tissue: activation of thermogenesis by Ca2+.* PloS one, 2010. **5**: p. e9439.

62. Brandl, C.J., et al., *Two Ca2+ ATPase genes: homologies and mechanistic implications of deduced amino acid sequences.* Cell, 1986. **44**: p. 597-607.

63. Zador, E., P. Vangheluwe, and F. Wuytack, *The expression of the neonatal sarcoplasmic reticulum Ca2+ pump (SERCA1b) hints to a role in muscle growth and development.* Cell Calcium, 2007. **41**: p. 379-388.

64. Wu, K.D. and J. Lytton, *Molecular cloning and quantification of sarcoplasmic reticulum Ca(2+)-ATPase isoforms in rat muscles.* Am J Physiol, 1993. **264**: p. C333-C341.

65. Pan, Y., et al., *Targeted disruption of the ATP2A1 gene encoding the sarco(endo)plasmic reticulum Ca2+ ATPase isoform 1 (SERCA1) impairs diaphragm function and is lethal in neonatal mice.* J Biol Chem, 2003. **278**: p. 13367-13375.

66. Mendler, L., et al., *Expression of sarcoplasmic/endoplasmic reticulum Ca2+ ATPases in the rat extensor digitorum longus (EDL) muscle regenerating from notexin-inducednecrosis.* J Muscle Res Cell Motil, 1998. **19**: p. 777-785.

67. Guglielmi, V., et al., *SERCA1 protein expression in muscle of patients with Brody disease and Brody syndrome and in cultured human muscle fibers.* Mol Genet Metab, 2013. **110**: p. 162-169.

68. Vihola, A., et al., *Altered expression and splicing of Ca(2+) metabolism genes in myotonic dystrophies DM1 and DM2.* Neuropathol Appl Neurobiol, 2013. **39**: p. 390-405.

69. Hoffman, E., et al., *Subcellular fractionation of dystrophin to the triads of skeletal muscle.* Nature, 1987. **330**: p. 754-758.

70. Hopf, F.W., et al., *A critical evaluation of resting intracellular free calcium regulation in dystrophic mdx muscle.* Am J Physiol, 1996. **271**: p. C1325-1339.

71. Altamirano, F., et al., *Increased resting intracellular calcium modulates NF-kappaB-dependent inducible nitric-oxide synthase gene expression in dystrophic mdx skeletal myotubes.* J Biol Chem, 2012. **287**: p. 20876-20887.

72. Imbert, N., et al., *Abnormal calcium homeostasis in Duchenne muscular dystrophy myotubes contracting in vitro.* Cell calcium, 1995. **18**: p. 177-186.

73. Alderton, J.M., *Calcium Influx through Calcium Leak Channels Is Responsible for the Elevated Levels of Calcium-dependent Proteolysis in Dystrophic Myotubes.* J Biol Chem, 2000. **275**: p. 9452-9460.

74. Lansman, J. and A. Franco-Obregón, *Mechanosensitive ion channels in skeletal muscle: a link in the membrane pathology of muscular dystrophy.* Clin Exp Pharmacol Physiol, 2006. **33**: p. 649-656.

75. Millay, D.P., et al., *Calcium influx is sufficient to induce muscular dystrophy through a TRPC-dependent mechanism.* Proc Natl Acad Sci U S A, 2009. **106**: p. 19023-19028.

76. Doran, P., et al., *Subproteomics analysis of Ca+-binding proteins demonstrates decreased calsequestrin expression in dystrophic mouse skeletal muscle.* Eur J Biochem / FEBS, 2004. **271**: p. 3943-3952.

77. Pertille, A., et al., *Calcium-binding proteins in skeletal muscles of the mdx mice: potential role in the pathogenesis of Duchenne muscular dystrophy.* Int J Exp Pathol, 2010. **91**: p. 63-71.

78. Ferretti, R., et al., *Sarcoplasmic-endoplasmic-reticulum Ca2+-ATPase and calsequestrin are overexpressed in spared intrinsic laryngeal muscles of dystrophin-deficient mdx mice.* Muscle Nerve, 2009. **39**: p. 609-615.

79. Goonasekera, S., et al., *Mitigation of muscular dystrophy in mice by SERCA overexpression in skeletal muscle.* J Clin Invest, 2011. **121**: p. 1044-1052.

80. Groenen, P. and B. Wieringa, *Expanding complexity in myotonic dystrophy.* Bioessays, 1998. **20**: p. 901-912.

81. Brook, J.D., et al., *Molecular basis of myotonic dystrophy: Expansion of a trinucleotide (CTG) repeat at the 3' end of a transcript encoding a protein kinase family member.* Cell, 1992. **68**: p. 799-808.

82. Fu, Y.H., et al., *An unstable triplet repeat in a gene related to myotonic muscular dystrophy.* Science, 1992. **255**: p. 1256-1258.

83. Mahadevan, M., et al., *Myotonic dystrophy mutation: an unstable CTG repeat in the 3' untranslated region of the gene.* Science, 1992. **255**: p. 1253-1255.

84. Liquori, C., et al., *Myotonic dystrophy type 2 caused by a CCTG expansion in intron 1 of ZNF9.* Science (New York, N.Y.), 2001. **293**: p. 864-867.

85. Kimura, T., et al., *Altered mRNA splicing of the skeletal muscle ryanodine receptor and sarcoplasmic/endoplasmic reticulum Ca2+-ATPase in myotonic dystrophy type 1.* Hum Mol Genet, 2005. **14**: p. 2189-2200.

86. Hino, S., et al., *Molecular mechanisms responsible for aberrant splicing of SERCA1 in myotonic dystrophy type 1.* Hum Mol Genet, 2007. **16**: p. 2834-2843.

87. Nakamori, M., et al., *Altered mRNA splicing of dystrophin in type 1 myotonic dystrophy.* Muscle Nerve, 2007. **36**: p. 251-257.

88. Salvatori, S., et al., *Comparative transcriptional and biochemical studies in muscle of myotonic dystrophies (DM1 and DM2).* Neurol Sci, 2009. **30**: p. 185-192.

89. Tago, H., H. Kimura, and T. Maeda, *Visualization of detailed acetylcholinesterase fiber and neuron staining in rat brain by a sensitive histochemical procedure.* J Histochem Cytochem, 1986. **34**: p. 1431-1438.

90. Kopniczky, Z., et al., *Lateral entorhinal cortex lesions rearrange afferents, glutamate receptors, increase seizure latency and suppress seizure-induced c-fos expression in the hippocampus of adult rat.* J Neurochem, 2005. **95**: p. 111-124.

91. Hall, Z.W. and R.B. Kelly, *Enzymatic detachment of endplate acetylcholinesterase from muscle.* Nat New Biol, 1971. **232**: p. 62-63.

92. McMahan, U.J., J.R. Sanes, and L.M. Marshall, *Cholinesterase is associated with the basal lamina at the neuromuscular junction.* Nature, 1978. **271**: p. 172-174.

93. Tidball, J.G., G. Salem, and R. Zernicke, *Site and mechanical conditions for failure of skeletal muscle in experimental strain injuries.* J Appl Physiol, 1993. **74**: p. 1280-1286.

94. Maier, A., *Contours and distribution of sites that react with antiacetylcholinesterase in chicken intrafusal fibers.* Am J Anat, 1989. **185**: p. 33-41.

95. Zádor, E., et al., *Expression of the sarco/endoplasmic reticulum Ca2+-transport ATPase protein isoforms during regeneration from notexin-induced necrosis of rat soleus muscle.* Acta Histochem, 1998. **100**: p. 355-369.

96. Zador, E., R. Fenyvesi, and F. Wuytack, *Expression of SERCA2a is not regulated by calcineurin or upon mechanical unloading in skeletal muscle regeneration.* FEBS Lett, 2005. **579**: p. 749-752.

97. Moss, F.P. and C.P. Leblond, *Satellite cells as the source of nuclei in muscles of growing rats.* Anat Rec, 1971. **170**: p. 421-435.

98. Vaittinen, S., et al., *Transected myofibres may remain permanently divided in two parts.* Neuromuscul Disord, 2002. **12**: p. 584-587.

99.    Grubb, B., J. Harris, and I. Schofield, *Neuromuscular transmission at newly formed neuromuscular junctions in the regenerating soleus muscle of the rat.* J Physiol, 1991. **441**: p. 405-421.

100.   Frank, E., et al., *The interaction between foreign and original motor nerves innervating the soleus muscle of rats.* J Physiol, 1975. **247**: p. 725-743.

101.   Brown, M.C., J.K. Jansen, and D. Van Essen, *Polyneuronal innervation of skeletal muscle in new-born rats and its elimination during maturation.* J Physiol, 1976. **261**: p. 387-422.

102.   Paul, A.C., *Muscle length affects the architecture and pattern of innervation differently in leg muscles of mouse, guinea pig, and rabbit compared to those of human and monkey muscles.* Anat Rec, 2001. **262**: p. 301-309.

103.   Rana, Z., M. Ekmark, and K. Gundersen, *Coexpression after electroporation of plasmid mixtures into muscle in vivo.* Acta Physiol Scand, 2004. **181**: p. 233-238.

104.   Davis, C.E., J.B. Harris, and L.V. Nicholson, *Myosin isoform transitions and physiological properties of regenerated and re-innervated soleus muscles of the rat.* Neuromuscul Disord, 1991. **1**: p. 411-421.

105.   Bureau, M.F., et al., *Intramuscular plasmid DNA electrotransfer: biodistribution and degradation.* Biochim Biophys Acta, 2004. **1676**: p. 138-148.

106.   Snow, M., *An autoradiographic study of satellite cell differentiation into regenerating myotubes following transplantation of muscles in young rats.* Cell Tiss Res, 1978. **186**: p. 535-540.

107.   Robertson, T.A., J.M. Papadimitriou, and M.D. Grounds, *Fusion of myogenic cells to the newly sealed region of damaged myofibres in skeletal muscle regeneration.* Neuropathol Appl Neurobiol, 1993. **19**: p. 350-358.

108.   Horsley, V., et al., *Regulation of the growth of multinucleated muscle cells by an NFATC2-dependent pathway.* J Cell Biol, 2001. **153**: p. 329-338.

109.   Bruusgaard, J.C., et al., *Number and spatial distribution of nuclei in the muscle fibres of normal mice studied in vivo.* J Physiol, 2003. **551**: p. 467-478.

110.   Morgan, J.E. and T.A. Partridge, *Muscle satellite cells.* Int J Biochem Cell Biol, 2003. **35**: p. 1151-1156.

111.   Bevan, S. and J.H. Steinbach, *The distribution of alpha-bungarotoxin binding sites of mammalian skeletal muscle developing in vivo.* J Physiol, 1977. **267**: p. 195-213.

112.   Mendler, L., et al., *mRNA levels of myogenic regulatory factors in rat slow and fast muscles regenerating from notexin-induced necrosis.* Neuromuscul Disord, 1998. **8**: p. 533-541.

113.   Zádor, E., L. Dux, and F. Wuytack, *Prolonged passive stretch of rat soleus muscle provokes an increase in the mRNA levels of the muscle regulatory factors distributed along the entire length of the fibers.* J Muscle Res Cell Motil, 1999. **20**: p. 395-402.

114.   de Meis, L., et al., *The thermogenic activity of rat brown adipose tissue and rabbit white muscle Ca2+-ATPase.* IUBMB life, 2005. **57**: p. 337-345.

115. Londraville, R.L., et al., *Cloning of a neonatal calcium atpase isoform (SERCA 1B) from extraocular muscle of adult blue marlin (Makaira nigricans).* Comp Biochem Physiol B Biochem Mol Biol, 2000. **127**: p. 223-233.

116. Dode, L., et al., *Low temperature molecular adaptation of the skeletal muscle sarco(endo)plasmic reticulum Ca2+-ATPase 1 (SERCA 1) in the wood frog (Rana sylvatica).* J Biol Chem, 2001. **276**: p. 3911-3919.

117. Pascual, M., et al., *The Muscleblind family of proteins: an emerging class of regulators of developmentally programmed alternative splicing.* Differentiation, 2006. **74**: p. 65-80.

118. Zhao, Y., et al., *Regulation of the alternative splicing of sarcoplasmic reticulum Ca(2)(+)-ATPase1 (SERCA1) by phorbol 12-myristate 13-acetate (PMA) via a PKC pathway.* Biochem Biophys Res Commun, 2012. **423**: p. 212-217.

119. Ho, T.H., et al., *Muscleblind proteins regulate alternative splicing.* EMBO J, 2004. **23**: p. 3103-3112.

120. Savkur, R.S., A.V. Philips, and T.A. Cooper, *Aberrant regulation of insulin receptor alternative splicing is associated with insulin resistance in myotonic dystrophy.* Nat Genet, 2001. **29**: p. 40-47.

121. Vihola, A., et al., *Histopathological differences of myotonic dystrophy type 1 (DM1) and PROMM/DM2.* Neurology, 2003. **60**: p. 1854-1857.

122. Zhao, X., et al., *Orai1 mediates exacerbated Ca(2+) entry in dystrophic skeletal muscle.* PLoS one, 2012. **7**: p. e49862.

123. Gayan-Ramirez, G., et al., *Corticosteroids decrease mRNA levels of SERCA pumps, whereas they increase sarcolipin mRNA in the rat diaphragm.* J Physiol, 2000. **524**: p. 387-397.

124. Williams, P.E. and G. Goldspink, *Longitudinal growth of striated muscle fibres.* J Cell Sci, 1971. **9**: p. 751-767.

125. Berendse, M., M.D. Grounds, and C.M. Lloyd, *Myoblast structure affects subsequent skeletal myotube morphology and sarcomere assembly.* Exp Cell Res, 2003. **291**: p. 435-450.

126. Horsley, V. and G. Pavlath, *Prostaglandin F2α stimulates growth of skeletal muscle cells via an NFATC2-dependent pathway.* J Cell Biol, 2003. **161**: p. 111-118.

127. Campbell, N.R., S.P. Podugu, and M.B. Ferrari, *Spatiotemporal characterization of short versus long duration calcium transients in embryonic muscle and their role in myofibrillogenesis.* Dev Biol, 2006. **292**: p. 253-264.

128. Takekura, H., B.E. Flucher, and C. Franzini-Armstrong, *Sequential docking, molecular differentiation, and positioning of T-Tubule/SR junctions in developing mouse skeletal muscle.* Dev Biol, 2001. **239**: p. 204-214.

129. Cusimano, V., et al., *Assembly and dynamics of proteins of the longitudinal and junctional sarcoplasmic reticulum in skeletal muscle cells.* Proc Natl Acad Sci U S A, 2009. **106**: p. 4695-4700.

130. Biehn, S.E., et al., *Expression of the sarco/endoplasmic Ca(2+)-ATPase, SERCA1a, in fibroblasts induces the formation of organelle membrane arrays.* Exp Cell Res, 2004. **292**: p. 78-88.

131. Lipskaia, L. and A.-M. Lompré, *Alteration in temporal kinetics of Ca2+ signaling and control of growth and proliferation.* Biol Cell, 2004. **96**: p. 55-68.

# ANNEX:

# Papers related to the thesis